Technical Report Documentation Page

1. Report No.	2. Government Accession No.	3. Recipient's Catalog No.
FHWA/TX-04/0-1816-1		

4. Title and Subtitle	5. Report Date
EVALUATION OF ROADSIDE SAFETY DEVICES USING FINITE ELEMENT ANALYSIS	April 2004 Resubmitted: August 2004
	6. Performing Organization Code
7. Author(s)	8. Performing Organization Report No.
Roger P. Bligh, Akram Y. Abu-Odeh, Mark E. Hamilton, and N. Ryan. Seckinger	Report 0-1816-1
9. Performing Organization Name and Address	10. Work Unit No. (TRAIS)
Texas Transportation Institute The Texas A&M University System College Station, Texas 77843-3135	11. Contract or Grant No. Project No. 0-1816
12. Sponsoring Agency Name and Address	13. Type of Report and Period Covered
Texas Department of Transportation Research and Technology Implementation Office P. O. Box 5080 Austin, Texas 78763-5080	Research: September 1998-August 2002
	14. Sponsoring Agency Code

15. Supplementary Notes

Research performed in cooperation with the Texas Department of Transportation and the U.S. Department of Transportation, Federal Highway Administration.
Research Project Title: Center of Excellence in DYNA3D Analysis (Crash Test Center)

16. Abstract

In recent years, roadside safety research efforts have focused on the utilization of computer simulation technology to gain a better understanding of the behavior of roadside safety devices when subjected to vehicular impact. The objective of this project was to utilize the resources of the Center for Transportation Computational Mechanics to support Texas Department of Transportation (TxDOT) roadside safety research.

The selection of roadside safety features to be modeled and simulated under this project was made in consultation with TxDOT personnel. Priority was given to modeling systems in support of ongoing, TxDOT- sponsored roadside safety projects. When design problems were identified through simulation or crash testing, researchers examined various design modifications to address the deficiencies and improve impact performance of the system. The results of the simulations were used to develop recommended improvements for full-scale crash testing and potential implementation.

Three distinct roadside safety issues were investigated with the aid of computer simulation. An alternative to the popular T6 tubular W-beam bridge rail was developed to address problems with vehicle instability observed in full-scale crash testing. A retrofit connection to TxDOT's grid-slot portable concrete barrier was developed to limit dynamic barrier deflections to levels more practical for work zone deployment. Finally, crashworthy mow strip configurations were developed for use when vegetation control around guard fence systems is desired to reduce the cost and risk associated with hand mowing.

17. Key Words	18. Distribution Statement
Finite Element Analysis, Roadside Safety, Computer Simulation, LS-DYNA, Bridge Rail, Portable Concrete Barrier, Guardrail, Mow Strip	No restrictions. This document is available to the public through NTIS: National Technical Information Service 5285 Port Royal Road Springfield, Virginia 22161

19. Security Classif.(of this report)	20. Security Classif.(of this page)	21. No. of Pages	22. Price
Unclassified	Unclassified	66	

Form DOT F 1700.7 (8-72) **Reproduction of completed page authorized**

EVALUATION OF ROADSIDE SAFETY DEVICES USING FINITE ELEMENT ANALYSIS

by

Roger P. Bligh, Ph.D., P.E.
Associate Research Engineer
Texas Transportation Institute

Akram Y. Abu-Odeh, Ph.D.
Associate Research Scientist
Texas Transportation Institute

Mark E. Hamilton
Graduate Assistant Researcher
Texas Transportation Institute

and

N. Ryan Seckinger
Graduate Assistant Researcher
Texas Transportation Institute

Report 0-1816-1
Project Number 0-1816
Research Project Title: Center of Excellence in DYNA3D Analysis
(Crash Test Center)

Sponsored by the
Texas Department of Transportation
In Cooperation with the
U.S. Department of Transportation
Federal Highway Administration

April 2004
Resubmitted: August 2004

TEXAS TRANSPORTATION INSTITUTE
The Texas A&M University System
College Station, Texas 77843-3135

DISCLAIMER

The contents of this report reflect the views of the authors, who are responsible for the facts and the accuracy of the data presented herein. The contents do not necessarily reflect the official view or policies of the Federal Highway Administration (FHWA) or the Texas Department of Transportation (TxDOT). This report does not constitute a standard, specification, or regulation. The engineer in charge was Roger P. Bligh, Ph.D., P.E., (Texas, # 78550).

ACKNOWLEDGMENTS

This research project was conducted under a cooperative program among the Texas Transportation Institute, the Texas Department of Transportation, and the U.S. Department of Transportation, Federal Highway Administration. The TxDOT project director for this research was Mr. Mark Marek, Design Division. His assistance and guidance are acknowledged and appreciated.

Portions of this work were co-sponsored by the Federal Highway Administration under Cooperative Agreement No. DTFH61-97-X-0029 "Development of Finite Element Models for Roadside Safety Applications." The authors wish to acknowledge the support and guidance of Mr. Martin Hargrave, FHWA, who served as the technical representative for those portions of the research.

TABLE OF CONTENTS

TABLE OF CONTENTS (CONTINUED)

Page

LIST OF FIGURES

LIST OF TABLES

CHAPTER 1. INTRODUCTION

Although significant advancements have been made over the past three decades, the roadside safety problem remains a major source of injury, death, and economic loss. According to the Transportation Research Board, as many as one million highway crashes occur on the roadside in the United States every year. One third of all highway fatalities are associated with these roadside crashes with annual societal costs exceeding $80 billion.

One of the most direct means of addressing this problem is through the continued development of improved roadside safety features. The design of roadside safety features presents many challenges and requires a thorough understanding of the complex interactions that occur in roadside crashes. For this reason, full-scale crash testing has been and continues to be the primary method for certifying the impact performance of roadside appurtenances. However, many research efforts have begun to integrate computer simulation of the impact event into the design, development, and evaluation process to better understand the behavior of the roadside safety device being impacted. One of the most widely used computer simulation codes for this purpose is LS-DYNA (*1*). LS-DYNA is a general purpose, nonlinear, explicit finite element code that was originally developed by Lawrence Livermore National Laboratory and has since been enhanced for automotive crash analysis by Livermore Software Technology Corporation (LSTC). Potential advantages of using sophisticated, state-of-the-art tools such as LS-DYNA in roadside safety research include design modification, optimization, and performance prediction. Utilization of these tools thereby minimizes the number of crash tests required to achieve compliance of a roadside safety device.

To help address the roadside safety problem, the Federal Highway Administration is actively supporting the use of LS-DYNA for the analytical simulation of roadside hardware impacts. In order to more fully develop and utilize the capabilities of this code, FHWA established "Centers of Excellence in DYNA3D Analysis" at selected universities and research agencies throughout the U.S. The Texas Transportation Institute (TTI) was awarded one of these national centers. Following this award, the Center for Transportation Computational Mechanics was established at TTI under joint funding by FHWA, TxDOT, TTI, and Texas A&M University. The purpose of the center is to contribute to the solution of the roadside safety problem through the use of computer simulation technology by building validated models of selected roadside hardware devices and establishing expertise in LS-DYNA that can be utilized by TxDOT, other highway agencies, and private industry to address safety problems. TTI researchers working under the center have actively pursued the integration of simulation into the roadside safety structure design and evaluation process.

PROJECT OBJECTIVE

The objective of this project was to utilize the resources of the Center for Transportation Computational Mechanics to support TxDOT roadside safety research. The purpose of the center is to develop and maintain a level of expertise in DYNA3D analysis such that it becomes

an integral part of the roadside safety structure design and evaluation process, thereby providing a unique resource to TxDOT and the nation for addressing critical roadside safety problems.

Research efforts being pursued through the center using finite element computer simulation include:

- re-evaluating existing hardware in response to changing impact performance criteria,
- developing new hardware to address problems identified with existing designs,
- optimizing existing systems to provide more cost-effective use of resources, and
- developing retrofit concepts to facilitate upgrading of existing hardware when necessary.

This project provided simulation support for ongoing roadside safety projects in areas where a more detailed understanding of the impact behavior was deemed useful in the evaluation and/or improvement of a device. Efforts focused on assessing compliance of existing roadside safety hardware with *National Cooperative Highway Research Program (NCHRP) Report 350* (*2*). When deficiencies were identified, simulation was used to assist in the development of improved and/or modified designs.

PROJECT SCOPE

The selection of roadside safety features to be modeled and simulated under this project is made in consultation with TxDOT personnel. Priority was given to modeling systems in support of ongoing, TxDOT-sponsored roadside safety projects. After the selection of a safety feature, researchers reviewed available literature and test data to examine failure mechanisms and identify critical components of the system, thus providing information regarding where to focus initial modeling and validation efforts.

Models for each key component or subsystem within the selected roadside safety feature were compared to experimental data to establish the accuracy and validity of each component. Full-scale load tests of selected components and materials were conducted to help quantify material properties and assist in the validation effort. The approach followed was to develop the system model from a series of validated component models.

Full-scale crash simulations were conducted on the system models using a detailed finite element model of a 4405-lb (2000-kg) pickup truck. The 4405-lb (2000 kg) pickup truck, denoted 2000P, is one of the design test vehicles recommended by *NCHRP Report 350*. The results of the initial full-scale simulations were used to evaluate the impact performance of the roadside safety feature.

When design problems were identified through simulation or crash testing, various design modifications were examined to address the deficiencies and improve impact performance of the system. This evaluation was accomplished by modifying the finite element model and conducting additional simulations to assess any improvement in impact performance. The results of the simulations were used to develop recommended improvements for full-scale crash testing and potential implementation.

The system initially selected for modeling and simulation was the T6 tubular W-beam bridge rail. Chapter 2 summarizes this effort, which provided support for research project 0-1804. Subsequent simulation work included analysis of TxDOT's grid-slot portable concrete barrier and evaluation of the practice of encasing guard fence in mow strips. Both of these simulation efforts were conducted in support of Research Project 0-4162, and the results are presented in Chapter 3 and Chapter 4, respectively. Chapter 5 of this report presents implementation recommendations.

CHAPTER 2. ANALYSIS OF THE TEXAS T6 BRIDGE RAIL SYSTEM

BACKGROUND

The Texas T6 bridge rail is a breakaway bridge rail system that is designed for use on culvert headwalls and thin bridge decks. Figure 1 shows a typical T6 bridge rail installation. The breakaway mechanism incorporated into the rail support posts helps minimize the transfer of large forces to the concrete deck, thus reducing the severity of deck damage during an impact.

Figure 1. T6 Bridge Rail Prior to Crash Test.

Since its original development in 1978, the Texas Type T6 bridge rail system has been widely used in Texas *(3)*. Primary components include a tubular W-beam rail element and W6×9 (W150×14) steel posts welded to steel baseplates that are bolted to the deck. The tubular rail is fabricated by welding two standard 12-gauge W-beam rails back-to-back using a 6-inch (150 mm) long intermittent skip weld. The two W-beam beam sections are staggered 15 inches (380 mm) in order to accommodate a bolted lap splice connection. The rail is mounted on W6×9 (W150×14) posts using 5/8-inch (16 mm) diameter button head bolts. A pipe sleeve is used between the tubular rail and post. The posts, which are spaced 75 inches (1.9 m) on center, connect to the baseplate with a breakaway weld detail. The baseplate is then anchored into or bolted through the concrete deck. The original breakaway weld connection was accomplished by

completely welding the tension flange, only slightly welding the inside of the compression flange, and providing no welds on the web.

The T6 system was originally tested under *Transportation Research Circular 191* and was later judged to be acceptable under *NCHRP Report 230* (*4*). This certification required full-scale crash testing of two scenarios: a 4500-lb (2041 kg) passenger vehicle impacting at a speed of 60 mph (96.5 km/h) and an angle of 25 degrees, and a 2250-lb (1020 kg) passenger vehicle impacting at a speed of 60 mph (96.5 km/h) and an angle of 15 degrees.

With the adoption of *NCHRP Report 350* (*2*), the T6 bridge rail required reevaluation. Test 3-11 of *NCHRP Report 350* requires a test involving a 4405-lb (2000 kg) pickup truck impacting the rail at a speed of 62.2 mph (100 km/h) and an angle of 25 degrees. In the first full-scale crash test (Test No. 418048-2) of the T6 bridge rail, the system did not perform satisfactorily (*5*). Although the bridge rail contained and redirected the vehicle, the vehicle rolled onto its side as it exited the installation.

A finite element model of the Texas T6 bridge rail system was developed to capture the performance trends of the existing T6 bridge rail system and evaluate potential design modifications. Several component models were validated on the subsystem level before the complete T6 finite element model was assembled. Proposed modifications to the T6 system were then modeled and evaluated. Details of this simulation effort are presented below.

DEVELOPMENT OF FINITE ELEMENT MODEL

Tubular Rail Element

Researchers observed in the full-scale crash tests that the tubular rail exhibited extensive crushing and deformation beyond the elastic limit. A piecewise linear plasticity material definition was, therefore, used to model the American Association of State Highway and Transportation Officials (AASHTO) M-180 guardrail steel using properties developed by Reid and Sicking (*6*). A failure strain was not specified since rupture or tearing of the rail was not expected nor observed in the full-scale crash tests.

Post/Baseplate Steel

Posts and baseplates used in the T6 system are fabricated from American Society for Testing and Materials (ASTM) A-36 grade steel. The American Institute of Steel Construction (AISC) *Load and Resistance Factor Design (LRFD)* design code defines this grade of steel as having a yield stress of 36 ksi (248 MPa) and a tensile stress capacity of 58 ksi (400 MPa). The difficulty arises in the fact that these specifications are merely minimum requirements. Much of the steel that is designated as A-36 is actually closer to grade 50 steel material. Grade 50 steel has a yield stress of 50 ksi (345 MPa) and a tensile stress capacity of 70 ksi (483 MPa).

To provide more accurate material data, researchers performed uniaxial tests of steel coupons cut from several W6×9 (W150×14) guardrail posts. The crosshead of the loading apparatus was periodically stopped during each test to measure the width and thickness of the specimens to assist with obtaining a true stress-strain curve for input into LS-DYNA.

Post-to-Baseplate Connections

During the full-scale crash test, the welded connection between the post and baseplate did not break away as designed. Static load tests on posts taken from the prototype rail installation showed that the capacity of the breakaway weld exceeded the plastic moment capacity of the post. This led to wheel snagging on the posts and significant deck damage. Therefore, to ensure consistent and reliable breakaway behavior, eliminate wheel snagging, and minimize deck damage, the post-to-baseplate connection was modified. Two slots were fabricated in the front tension flange to induce ductile failure in the post material at a controlled load rather than rely on fracture of the weld. Further, the length of the welds on the inside of the back compression flange was reduced. To prevent hinging of the post about these rear welds, a doubler plate was welded to the back side of the compression flange. This plate induces tensile loads in the welds on the compression flange, which fail the welds and permit complete release of the post from the baseplate. To reduce deck damage, the size of the baseplate was increased to 12 inches (305 mm) × 9 1/2 inches (241 mm) × 1 inch (25 mm) as shown in Figure 2.

Two pendulum tests were conducted to evaluate the behavior of the modified post-to-baseplate connection – one along the strong axis of the post and the other along the weak axis of the post. The pendulum was outfitted with a crushable honeycomb nose assembly that simulates the frontal crush stiffness of a small passenger car. The impact speed for the pendulum tests was nominally 21.7 mph (35 km/h). During the strong-axis impact, the post completely broke away from the baseplate as designed. In the weak axis direction, the post hinged and did not release. Such weak-axis behavior is desired in order to resist longitudinal rail forces imparted to the posts through the post connection bolts.

Simulating these pendulum tests validated the model. Figures 3 and 4 show a comparison of the pendulum tests to the simulations for impacts about the strong and weak axis of the post, respectively. The measured acceleration signals obtained from the pendulum tests were compared to those obtained from the LS-DYNA simulations. The comparison for the strong and weak axis tests is shown in Figures 5(a) and 5(b), respectively.

As shown in these plots, test and simulation signals have similar characteristics in terms of phase, peak amplitude, and duration of impact. Moreover, the behavior of the post in terms of release and trajectory during simulations was similar to the behavior observed in the pendulum tests. Therefore, the post model and its connection to the baseplate were considered valid.

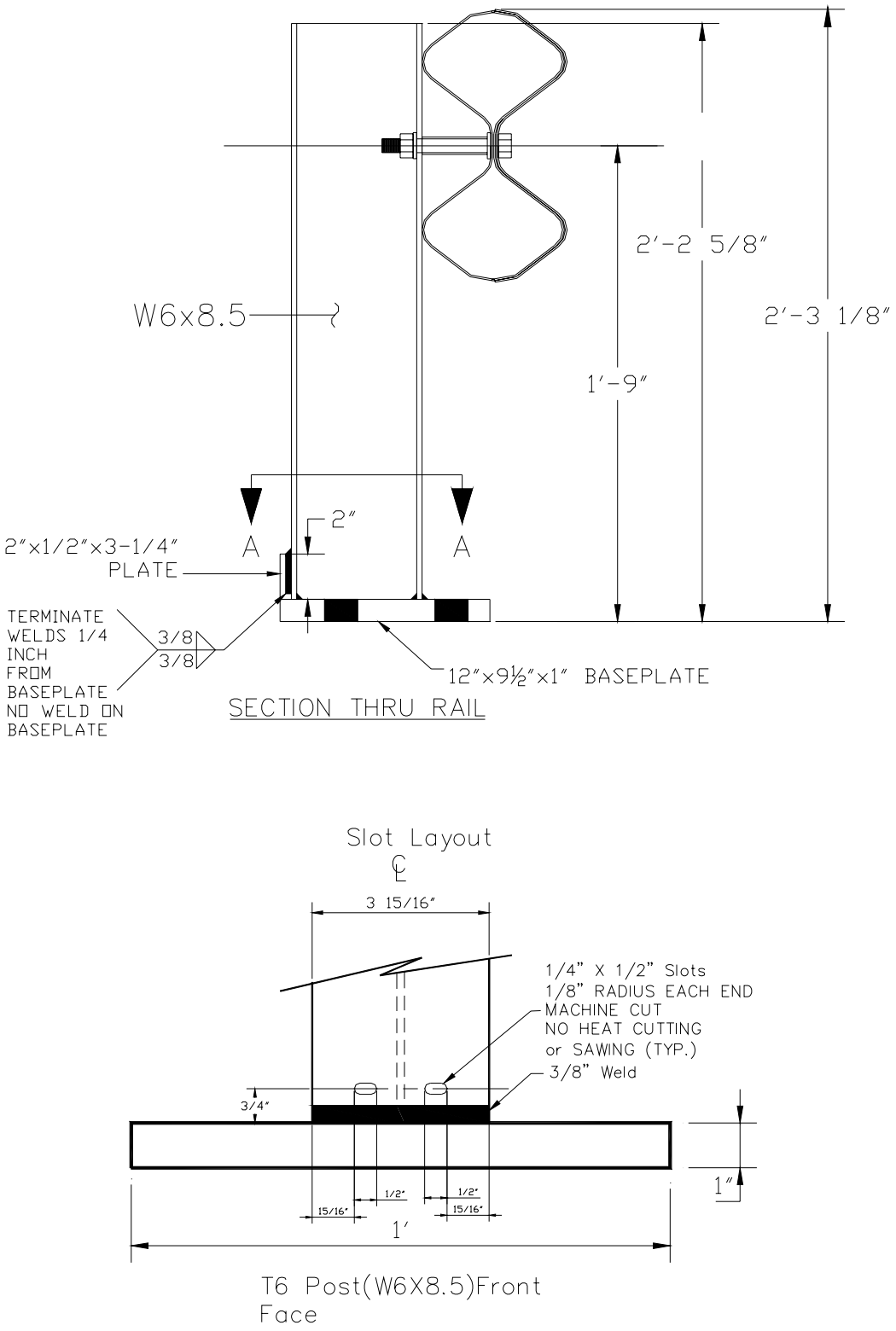

Figure 2. Details of Modified Post-to-Baseplate Connection.

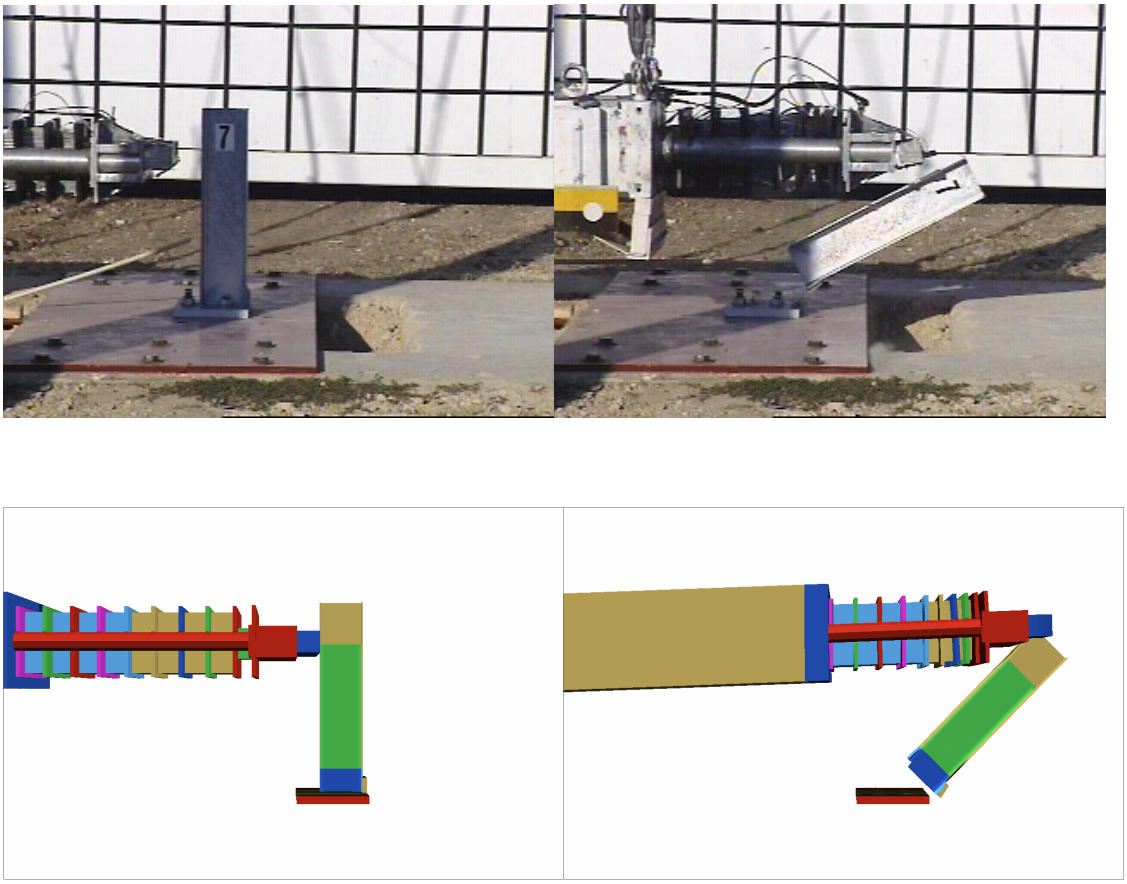

Figure 3. Comparison of Test and Simulation for Strong Axis Post Impact.

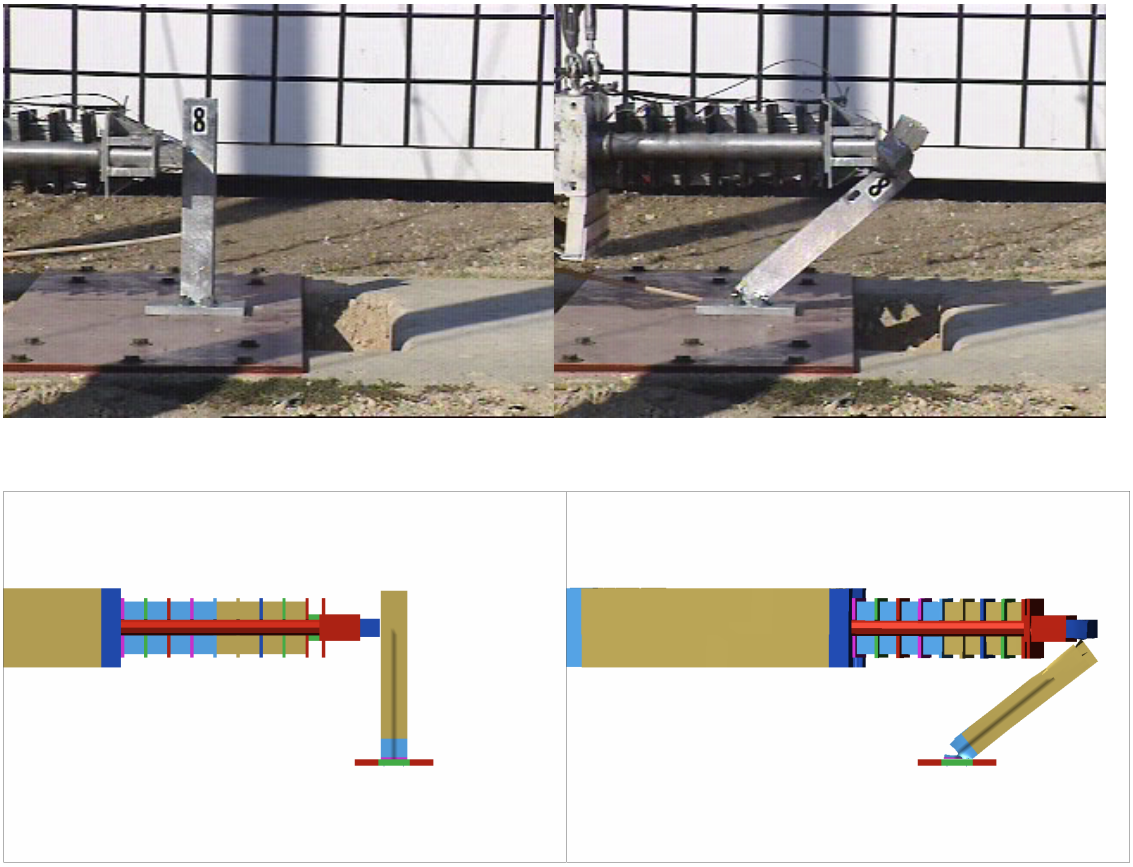

Figure 4. Comparison of Test and Simulation for Weak Axis Post Impact.

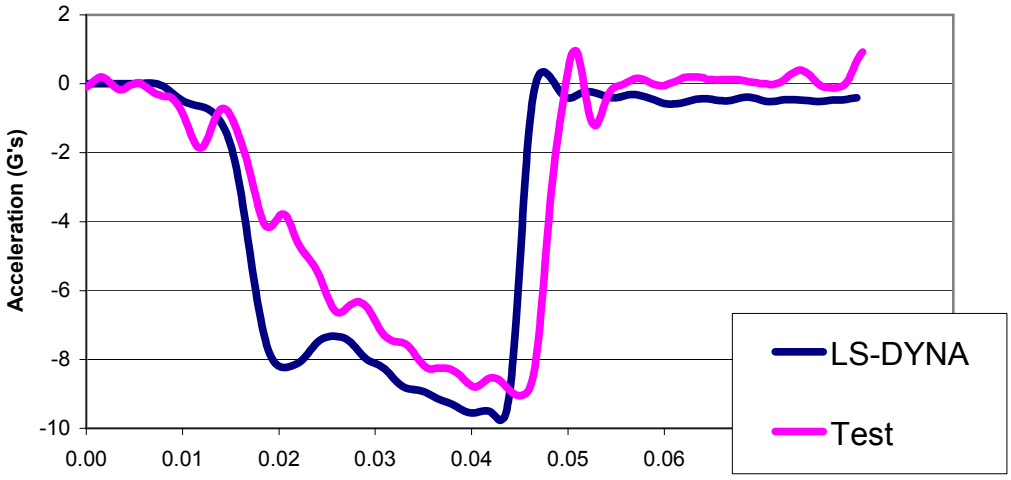

(a) Strong Axis.

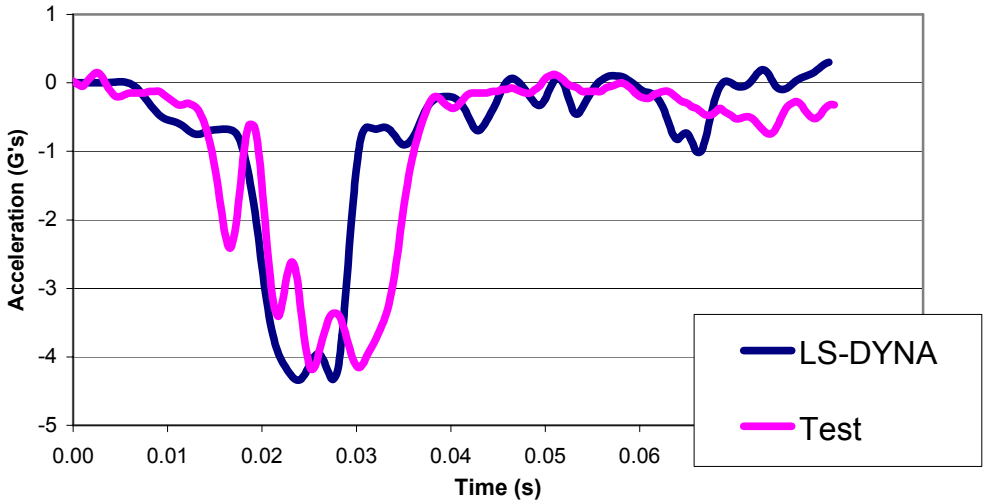

(b) Weak Axis.

Figure 5. Comparison of Pendulum Test Acceleration Signals.

Post-to-Rail Connection

As shown in Figure 2, a 5/8-inch (16 mm) diameter button head bolt is used to connect the tubular W-beam rail to the flange of the W6×9 (W150×14) steel post. Unlike a standard W-beam guardrail, the valley of the tubular W-beam element through which the connection is made is offset from the face of the post approximately 3.0 inches (75 mm). A 1-1/4-inch (32 mm) diameter pipe sleeve is used to span this gap.

Many previous modeling efforts involving W-beam guardrails approximate the post-to-rail connection with spring elements. However, because the post-to-rail connection used on the T6 bridge rail system is offset from the valley of the W-beam, the connecting bolt experiences axial, shear, and bending loads. Modeling the post-to-rail connection using springs would not have captured the combined loading effects. Therefore, the post-to-rail connection in the finite element model was modeled using beam elements whose cross section and strength were based on the characteristics of the bolted assembly.

Baseplate-to-Concrete Deck Connection

Four 1-1/2-inch (32 mm) diameter anchor bolts connect the baseplate of the T6 bridge rail is connected to the concrete deck. The resulting constraint on the base was modeled by fixed boundary conditions placed on nodes corresponding to the geometric centers of the anchoring bolts. During the full-scale crash tests, the concrete bridge deck suffered extensive cracking and damage due to punching shear. As expected, most damage was localized around the post locations. Current material models contained within LS-DYNA are not capable of accurately modeling concrete damage and failure of this type. The development of such a model is the subject of ongoing research sponsored by FHWA. Consequently, the concrete deck for the T6 bridge rail was represented by rigid shell elements. The deck drop-off behind the T6 installation was incorporated into the model to account for any effect it might have on vehicle response.

Determination of Boundary Conditions for Rail Ends

Another issue addressed in the modeling effort was the determination of appropriate boundary conditions for the ends of the tubular W-beam rail. In the full-scale crash test, the end treatment consisted of a 12.5-ft (3.8 m) section of strong post W-beam approach guardrail attached to a 37.5-ft (11.4 m) long LET guardrail end treatment. The goal was to represent the axial stiffness of the combined approach guardrail and end treatment as boundary conditions at the free ends of the bridge rail.

A finite element model of the approach guardrail and end treatment was developed and subjected to an axial load at the free end of the approach guardrail. The results of these simulations were used to find a force-displacement curve that corresponded to the stiffness of the combined guardrail and end treatment. These properties were assigned to shell elements that were connected around the perimeter of the free ends of the front rail member of the tubular W-beam to represent the unsymmetrical attachment of the approach rail to the tubular W-beam.

COMPARISON OF SIMULATION TO FULL-SCALE CRASH TEST

As previously referenced, a full-scale crash test of the T6 bridge rail system was conducted following the prescribed impact conditions for *NCHRP Report 350* Test 3-11 (*7*). All LS-DYNA modeling efforts reported herein were intended to simulate this specific test. The test consisted of a 4405-lb (2000 kg) Chevrolet pickup truck impacting the Texas Type T6 bridge rail 35.4 inches (900 mm) upstream from the splice at post 11 at a speed of 61.8 mph (99.5 km/h) and an angle of 27.0 degrees. Figure 6 shows a photo of the T6 installation after this test.

Figure 6. Rail Damage from Tubular W-beam Crash Test.

Version 9 of the C2500 pickup truck model was obtained from the National Crash Analysis Center (NCAC) for incorporation into the simulation (*8*). This version of the pickup model has improved tire meshing, explicit rear suspension, rear bumper, and better side meshing among other improvements over previous releases.

A simulation was conducted with the revised vehicle model and the T6 tubular W-beam bridge rail model. Figure 7 shows a downstream view of both test and simulation of the pickup truck impacting the T6 bridge rail. The simulation shows close similarities with the crash test for the first 200 milliseconds (ms). After this time, there was a gradual separation between crash test and simulation signals. However, various aspects of the simulations and test continued to compare favorably up to 500 ms.

(a) Test and Simulation at 0.0 s.

(b) Test and Simulation at 0.060 s.

(c) Test and Simulation at 0.493 s.

Figure 7. Comparison of Tubular W-beam Test and Simulation.

Although the pickup truck in the simulation did not roll over, it did exhibit a behavioral trend similar to the vehicle tested. Table 1 shows a comparison between the crash test and LS-DYNA simulation of the T6 tubular W-beam. It indicates that the simulation captured most of the crash test characteristics in terms of number of posts broken, time of backslap and exit speed. Both the crash test and the simulation results indicate that the T6 rail system does not provide adequate height for preventing rollover of the pickup truck. Standard guardrail and rigid bridge rail systems with similar heights (27 inches [686 mm]) have passed *NCHRP Report 350* criteria without inducing rollover of the vehicle. However, these rail systems maintain or stay close to their original height upon impact, whereas the T6 system loses its initial height once posts start breaking. Moreover, the existence of the deck drop-off behind the rail may have aggravated the roll motion of the vehicle.

Table 1. Comparison of Tubular W-beam Crash Test and Simulation.

	Crash Test	LS-DYNA Simulation
Maximum dynamic rail deflection	3.0 ft (0.9 m)	2.6 ft (0.8 m)
Maximum static rail deflection	2.6 ft (0.8 m)	2.1 ft (0.6 m)
Number of posts broken	5	5
Backslap time	0.247 s	0.245 s
Vehicle exit conditions		
Speed	40.3 mph (64.8 km/h)	40.9 mph (65.8 km/h)
Angle	27.7 deg	15 deg

SIMULATION OF MODIFIED T6 (TUBULAR THRIE-BEAM SYSTEM)

Given the unsuccessful performance of the T6 tubular W-beam bridge rail, the researchers investigated changes to the system to enhance its performance. As mentioned in the previous paragraph, the research team linked the instability of the vehicle (i.e., rollover) to the height of the rail system. Increasing the height of the rail system should improve performance in terms of vehicle stability. Hence, an alternative design to the tubular W-beam rail system is a tubular thrie-beam rail system. The tubular thrie-beam system is fabricated by welding two sections of thrie-beam rail back to back in a manner similar to that used in the fabrication of the tubular W-beam.

The mounting height of thrie-beam rail is 31 inches (788 mm) compared to 27 inches (689 mm) for the W-beam rail height. The thrie-beam rail section is 20 inches (510 mm) deep compared to the 12-1/4 inches (312 mm) deep W-beam rail section. This places the bottom of the thrie-beam at 11 inches (279 mm) compared to approximately 15 inches (381 mm) for W-beam. Therefore, there are no concerns related to a small car underriding the taller rail.

It should be noted that the height of the applied impact loads on the taller tubular thrie-beam rail will be greater than for the tubular W-beam rail. This will induce greater bending moment in the posts which, in turn, will result in more posts failing and breaking away from their baseplates. Although the strength of the post could be adjusted, a more direct comparison of

the effect of rail height was desired and, therefore, the post model was left unchanged other than to increase the post height to accommodate the taller rail.

Figure 8 shows sequential images for the LS-DYNA simulation with the tubular thrie-beam rail system. As expected, more posts were knocked out in the simulation of the tubular thrie-beam than in the tubular W-beam simulation. The vehicle was more stable and exhibited a relatively small maximum roll angle (18-20 degrees). This provides a strong indication that the tubular thrie-beam system has a high probability of passing *NCHRP Report 350* test 3-11 requirements. Additional results of the simulation are shown in Table 2.

Figure 8. Tubular Thrie-beam Simulation Sequence.

Table 2. Simulation Results for Tubular Thrie-beam Rail.

Maximum dynamic rail deflection	3.45 ft (1.1 m)
Maximum static rail deflection	N/A
Number of posts broken	12
Backslap time	0.266 s
Max roll angle	18.5 deg

CONCLUSIONS AND RECOMMENDATIONS

The primary objective of this research was the development of an accurate finite element model of the T6 bridge rail system using the explicit LS-DYNA code and modifications to the T6 system that would address the rollover problem with the existing design. Several component models were validated on the subsystem level before the complete T6 finite element model was assembled. Final simulations involving impact of a 4405-lb (2000 kg) truck model under TL-3 conditions showed reasonable correlation with crash test results. The amount of deformation experienced by the vehicle and the T6 model, the overall trajectory of the vehicle, and exit velocity were several of the evaluation criteria that correlated well with recorded data from the full-scale crash test. Although the vehicle experienced a high roll angle, it did not ultimately roll over as observed in the crash test. This discrepancy is likely attributed to several factors, including the frictional contact between the vehicle and the rail system, the inertial properties of the vehicle model, and the representation of the suspension/steering systems in the vehicle model.

A modified T6 system that incorporates a tubular thrie-beam rail element instead of the original tubular W-beam was modeled and simulated. During this simulation, the vehicle experienced significantly less roll angle than the simulation with the tubular W-beam. More posts failed due to the higher loading applied by the taller tubular thrie-beam rail. This tubular thrie-beam bridge rail system has a good probability of passing *NCHRP Report 350* Test Level 3 requirements if crash tested.

The performance of the tubular thrie-beam system could be improved prior to testing by redesigning the post baseplate connection to increase its strength. The strength values should be chosen to reduce the number of posts broken to a total of six or seven posts. This would limit travel of the vehicle over the edge of the deck, which might further reduce the vehicle roll angle. Maintenance and repair costs would also be reduced.

CHAPTER 3. EVALUATION OF TEXAS GRID-SLOT PORTABLE CONCRETE BARRIER SYSTEM

BACKGROUND

The impact performance of many roadside safety features has had to be reevaluated to demonstrate compliance with *NCHRP Report 350*. TxDOT sponsored research project 0-4162 to investigate various barrier performance and placement issues. Among the appurtenances selected for testing and evaluation was TxDOT's Type 2 precast concrete traffic barrier (PCTB[1]-90) with joint type A.

This commonly used portable barrier system consists of precast segments that are 30 ft (9.1 m) in length and have a standard New Jersey safety shape profile. The barrier segments are 2 ft-8 inches (0.8 m) in height, 2 ft-3 1/4 inches (0.7 m) wide at the base, and 8 inches (203 mm) wide at the top. The joint connection involves placing a prefabricated tiebar grid into a slot formed into the end of the adjacent barrier segments. The slots are 2 inches (51 mm) wide, 9 inches (229 mm) long, and extend to a depth of approximately 22 inches (559 mm) from the top of the barrier. The segments are connected by aligning slots formed into the ends of adjacent concrete barrier segments and inserting a prefabricated tiebar grid into the slot. The 18-inch (457 mm) square steel bar grid is fabricated from three 1-inch (25 mm) diameter steel tiebars in the horizontal direction and two 1/2-inch (13 mm) diameter tiebars in the vertical direction. TxDOT standard drawings PCTB(1)-90 and PCTB(2)-85 entitled "Precast Concrete Traffic Barrier Type 2" provide additional information on the barrier segments and steel bar connection grid.

Although the TxDOT Type 2 precast concrete traffic barrier has reportedly worked well in the field, the crash performance of the barrier with respect to the *NCHRP Report 350* guidelines was unproven. A full-scale crash test was therefore conducted to evaluate the impact behavior of the barrier (*9*). The test article for the crash test consisted of standard, unmodified precast concrete barrier segments as detailed in TxDOT standard drawings. However, the standard steel bar grid used to connect the segments was replaced with an 18 inches × 18 inches × 3/4 inch (457 mm × 457 mm × 19 mm) thick steel plate. Three pieces of #6 (#19) reinforcing steel were welded to the plate to provide an overall thickness equivalent to that of the standard steel bar grid and reduced the play of the connector in the precast slots in the barrier segments. The intent of substituting the steel plate for the steel bar grid was to ensure the full strength of the concrete was utilized at the joints.

The modified Texas grid-slot portable concrete barrier with steel connector plate met *NCHRP Report 350* evaluation criteria. Although one of the barrier joints separated, the test vehicle was contained and redirected. However, TxDOT desired further reduction of the maximum dynamic barrier deflection.

OBJECTIVES/SCOPE OF RESEARCH

The impact performance of temporary concrete barriers is influenced by a number of variables that include but are not limited to: barrier profile, barrier height, segment length, joint rotation slack, joint moment capacity, joint tensile strength, and barrier-roadway friction. The design of the joint connection plays a particularly critical role in the impact performance of temporary concrete barriers. The design of the joint has a direct influence on the magnitude of lateral barrier deflection and degree of barrier rotation during a vehicular impact event. A joint with inadequate strength and/or stiffness can induce instability of the vehicle and/or result in failure of the connection and penetration of the vehicle through the barrier.

The objective of this research was to develop a retrofit connection for the Texas grid-slot portable concrete barrier that limits dynamic deflections to more practical levels during design impact events. This work supported TxDOT Research Project 0-4162. TxDOT engineers and TTI researchers jointly conceptualized several retrofit connection designs. When developing the retrofit design options, factors such as impact performance, cost, ease of field installation, and aesthetics were considered.

The research team performed various analyses to help assess the ability of the selected barrier systems to meet *NCHRP Report 350* impact performance criteria prior to conducting the full-scale crash testing. Computer simulation techniques supported the analysis efforts. The simulation provided a more detailed understanding of the three-dimensional impact response of the barrier design. The program utilized in the computer modeling efforts was LS-DYNA. LS-DYNA is a general-purpose, explicit finite element code used to analyze the nonlinear dynamic response of three-dimensional inelastic structures. Limitations in the ability of existing material models to accurately capture concrete fracture and failure led to some simplifying assumptions regarding the model of the grid-slot connection. Nonetheless, the simulations assisted in the impact performance evaluation of the existing and modified designs.

ALTERNATE CONNECTION DESIGNS

Although the barrier evaluated in the first crash test met *NCHRP Report 350* evaluation criteria, further reduction of the maximum dynamic barrier deflection was desired. As evidenced by the concrete failure of the walls of the slotted barrier ends in the crash test, the barrier segments did not possess any additional moment capacity at the joint that could be utilized to reduce deflections. Therefore, various retrofit concepts were explored to introduce tensile capacity across the joints.

Computer simulations of full-scale barrier impacts were performed to help evaluate the relative improvement in dynamic deflection provided by two different connection alternatives: a U-bar connector and steel straps. The simulations were conducted in a predictive manner and full-scale crash tests of the modified barrier systems were subsequently run under Research Project 0-4162. Details of the simulation and testing are summarized below.

U-bar Connection with Rebar Grid

The first concept that TxDOT elected to evaluate involved using a "U-shaped" bar across the barrier joints to connect the barrier segments. The retrofit connection involved drilling a 1-3/4-inch (44 mm) diameter hole vertically into each barrier segment near the inside end of the precast slot. No other modifications were made to the barrier segments. A U-bar was bent from 1-1/2-inch (38 mm) diameter steel bar stock. The 6-inch (152 mm) legs of the U-bar were inserted into the predrilled holes in adjacent ends of two barrier segments. The U-bar was welded to the bottom of a modified steel bar grid that was fabricated from six #8 (#25) reinforcing bars in the horizontal direction and two #4 (#13) reinforcing bars in the vertical direction. The total weight of the steel bar grid and U-bar was approximately 39 lb (17.7 kg).

In order to investigate the effectiveness of the U-bar connection in reducing dynamic deflections, a finite element model of the modified grid-slot portable concrete barrier (PCB) with U-bar connections was developed. The PCB was modeled with brick elements to provide a geometrically representative cross section in accordance with the dimensions shown in TxDOT standard drawing PCTB(2)-85. Elements in the bottom 3 inches (75 mm) of the barrier were assigned elastic properties, while the remainder of the elements comprising the barrier cross section were assigned rigid material properties.

The U-bar and rebar grid were assigned appropriate deformable steel material properties using a piecewise linear plasticity model. The material properties assigned to the U-bars were consistent with an ASTM A-36 material, while those assigned to the rebar grid conformed to Grade 60 reinforcing steel. Due to the lack of reinforcement in and around the walls of the concrete barrier sections, researchers recognized that the tensile capacity of the U-bar connection was limited by the shear strength of the concrete beneath the precast slot. As mentioned previously, current material models contained within LS-DYNA are not capable of accurately modeling concrete damage and failure. An engineering analysis was performed to determine the ultimate shear strength of the concrete resisting the pull out of the U-bar connector. The surface area of the failure plane was determined using 3-dimensional drawings of the barrier. The associated failure force was assigned to a portion of the U-bar connector. Thus, failure of the connection was modeled to occur in the U-bar at a level of force consistent with the ultimate strength of the concrete. Figure 9 shows the finite element representations of the U-bar connector and rebar grid.

Full-Scale Simulation

Several full-scale LS-DYNA simulations were conducted on the grid-slot portable concrete barrier model with U-bar connectors. The completed model consisted of six 30-ft (9.1 m) concrete barrier segments with five joints for a total barrier length of 180 ft (55 m). The results of the simulation were used to assess the effectiveness of the retrofit U-bar connections in reducing dynamic barrier deflections.

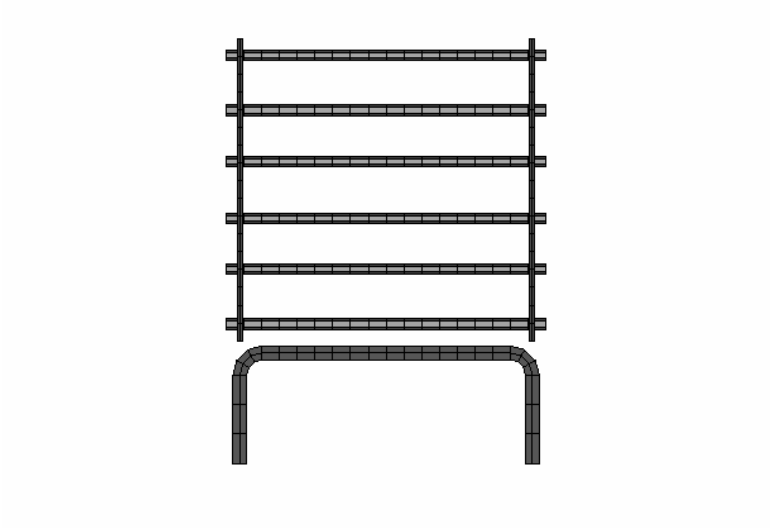

Figure 9. Finite Element Models of U-bar Connector and Rebar Grid.

The impact conditions for the simulations followed those of *NCHRP Report 350* Test Designation 3-11. This test involves a 4405-lb (2000 kg) pickup truck impacting the barrier at 62 mph (100 km/h) and 25 degrees. The impact location was selected to be 3.9 ft (1.2 m) upstream from the sixth barrier joint, which is consistent with the critical impact point recommended in *NCHRP Report 350*. The reduced pickup truck model developed by the National Crash Analysis Center was used in the simulations. Figure 10 shows an image of the barrier and vehicle model.

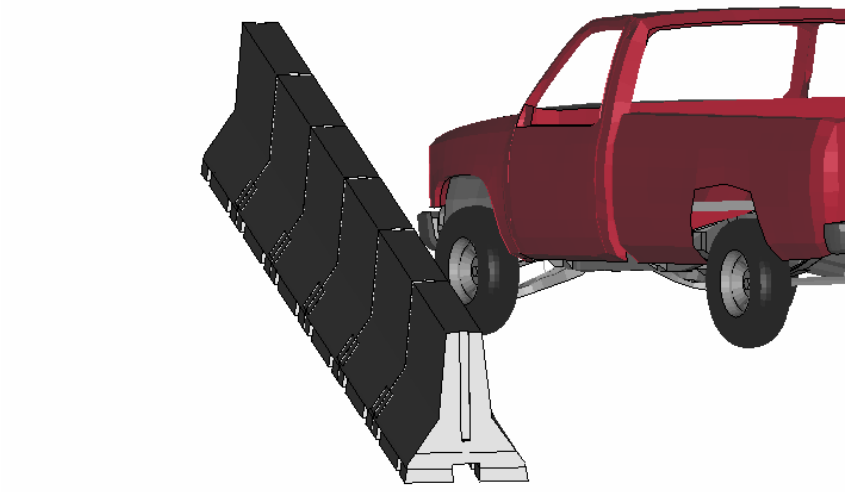

Figure 10. Finite Element Model of Grid-Slot PCB with U-bar Connectors.

The simulations indicated that the barrier segments lacked the strength to maintain connection integrity. The U-bar connection at the joint immediately downstream from the point of impact failed, resulting in large lateral barrier deflections. As noted above, the failure of the U-bar connector was indicative of a pull-out failure of the bar due to shear failure of the concrete at the base of the barrier below the precast grid-slot.

Full-Scale Crash Test

Although the analyses indicated high lateral barrier deflections due to loss of integrity of the U-bar connection under design impact conditions, TxDOT elected to test the system because the U-bar option was much more cost effective than the other proposed retrofit designs. The U-bar connector also provides a convenient drop-in type connection that greatly simplifies field installation and thereby reduces the exposure of workers. Therefore, a crash test with the U-bar connector was conducted to see if the available concrete strength was sufficient to reduce dynamic barrier deflections.

The test installation consisted of six barrier segments connected together for a total test installation length of approximately 180 ft (55 m). Figure 11 shows photographs of the completed test installation. Additional details of the test can be found in reference (*9*).

The modified Texas grid-slot portable concrete barrier with U-bar connector and rebar grid met all required *NCHRP Report 350* evaluation criteria. However, although the test vehicle was contained and redirected, barrier separation occurred at the two joints immediately downstream of the point of impact. Although the U-bar connector provided tensile capacity across the joints, this tensile capacity was limited by the shear strength of an unreinforced section of concrete beneath the precast slot. After failure of this concrete block and the walls forming the slot, integrity of the connections was lost and the barrier ends experienced a maximum lateral barrier movement of 12.4 ft (3.8 m). Photographs of the damaged barrier after the test are shown in Figure 12.

Steel Strap with Rebar Grid

Since the limited concrete capacity rendered the U-bar treatment ineffective in terms of reducing dynamic barrier deflection, another retrofit concept was evaluated. The treatment consisted of bolting 4-inch (102 mm) wide, 3/16-inch (5 mm) thick steel straps across the barrier joints on both the front and back sides of the barrier. Two 1-1/4 inch × 2-1/2 inch (32 mm × 64 mm) slotted holes are fabricated into each end of the 48-inch (1219 mm) long straps. The straps are anchored to the sloped face of the toe of each safety-shaped barrier using two sleeve anchors embedded approximately 7 inches (178 mm). The anchors were located approximately 8-1/4 inches (210 mm) from the base of the barrier and were spaced 9 inches (229 mm) apart. A rebar grid similar to that used with the U-bar connector was placed in the precast slots in the barrier end in conjunction with the steel straps.

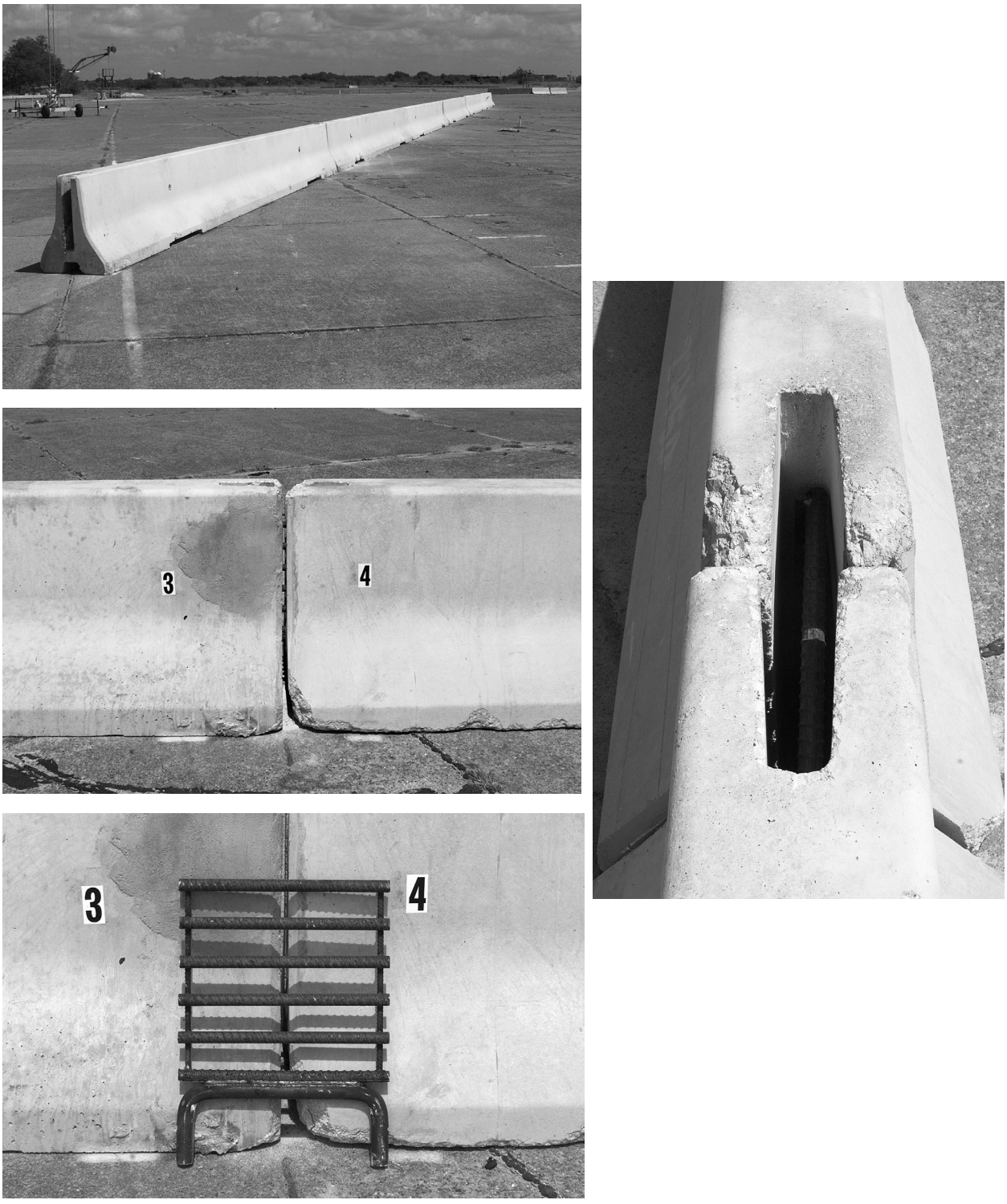

Figure 11. Grid-Slot Barrier with U-bar Connector Before Crash Test.

Figure 12. Grid-Slot Barrier with U-bar Connector After Crash Test.

In order to investigate the effectiveness of the steel straps in reducing dynamic deflections, a finite element model of the modified grid-slot portable concrete barrier with steel straps and rebar grid was developed. The PCB model used in the investigation of the U-bar connection was modified to incorporate the steel straps.

The steel straps and rebar grid were assigned appropriate deformable steel material properties using a piecewise linear plasticity model. The material properties assigned to the steel straps were consistent with an ASTM A-36 material, while those assigned to the rebar grid conformed to Grade 60 reinforcing steel. The steel strap was assigned a plastic failure strain of 0.26 to capture a ductile tensile mode of failure. The anchor bolts were not explicitly modeled but rather were represented by constraining selected nodes of the steel straps to the barrier using a tied nodes-to-surface contact definition. Since the anchor bolts were designed to have a shear strength that exceeded the tensile capacity of the steel straps, failure of the anchor bolts was not modeled. However, the section forces in the steel straps were monitored during the simulations and to confirm that the shear capacity of the bolts would not be exceeded.

Full-Scale Simulation

Several full-scale LS-DYNA simulations were conducted on the grid-slot portable concrete barrier model with steel strap retrofit. The completed model consisted of six 30-ft concrete barrier segments with five joints for a total barrier length of 180 ft. The results of the simulation were used to assess the effectiveness of the retrofit steel straps in reducing dynamic barrier deflections.

The impact conditions for the simulations followed those of *NCHRP Report 350* Test Designation 3-11. This test involves a 4405-kg (2000 kg) pickup truck impacting the barrier at 62 mph (100 km/h) and 25 degrees. The impact location was selected to be 3.9 ft (1.2 m) upstream from the sixth barrier joint, which is consistent with the critical impact point recommended in *NCHRP Report 350*. Figure 13 shows an image of the finite element barrier model.

Results of the computer simulation indicated that the tensile capacity provided by the steel straps should significantly reduce dynamic barrier deflections. Figure 14 shows the simulated barrier after impact. The maximum lateral barrier movement estimated from the simulations was 3.5 ft (1.1 m). Since the barrier model did not explicitly account for concrete failure in the walls at the ends of the barrier segments, researchers recognized that the actual deflections might be higher than predicted. However, since the estimated deflection represented a significant improvement from the deflections observed in the previous tests of the grid-slot portable concrete barrier, TxDOT made the decision to conduct a full-scale crash test of the steel strap retrofit design.

Time = 0 s

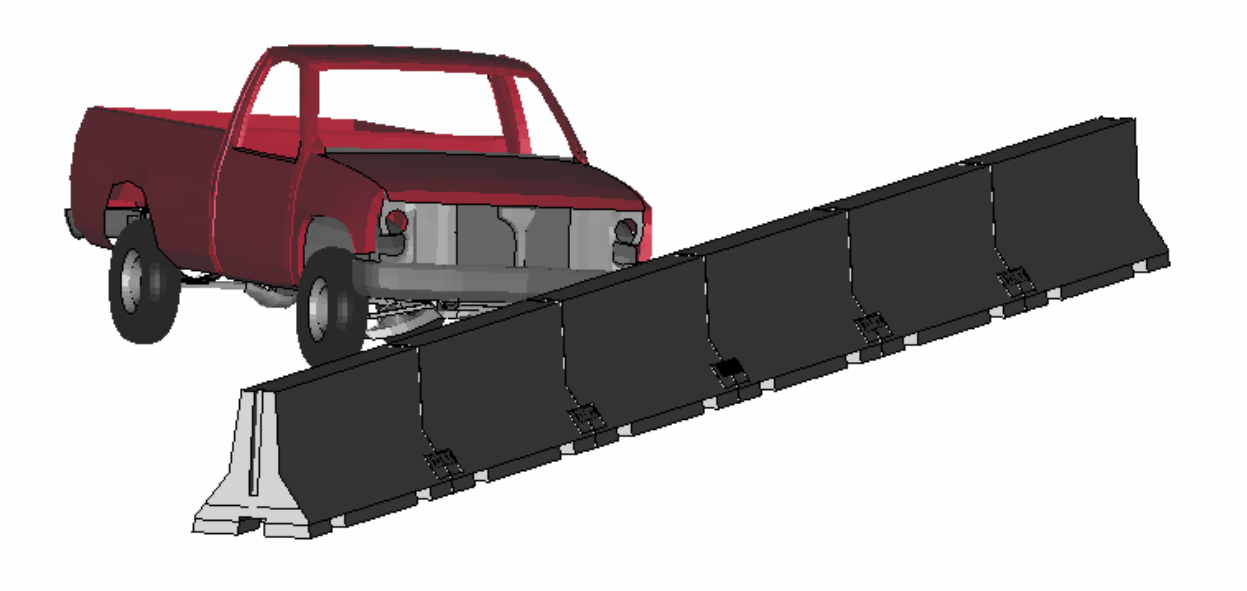

Figure 13. Finite Element Model of Grid-Slot PCB with Steel Straps.

Time = 0.5 s

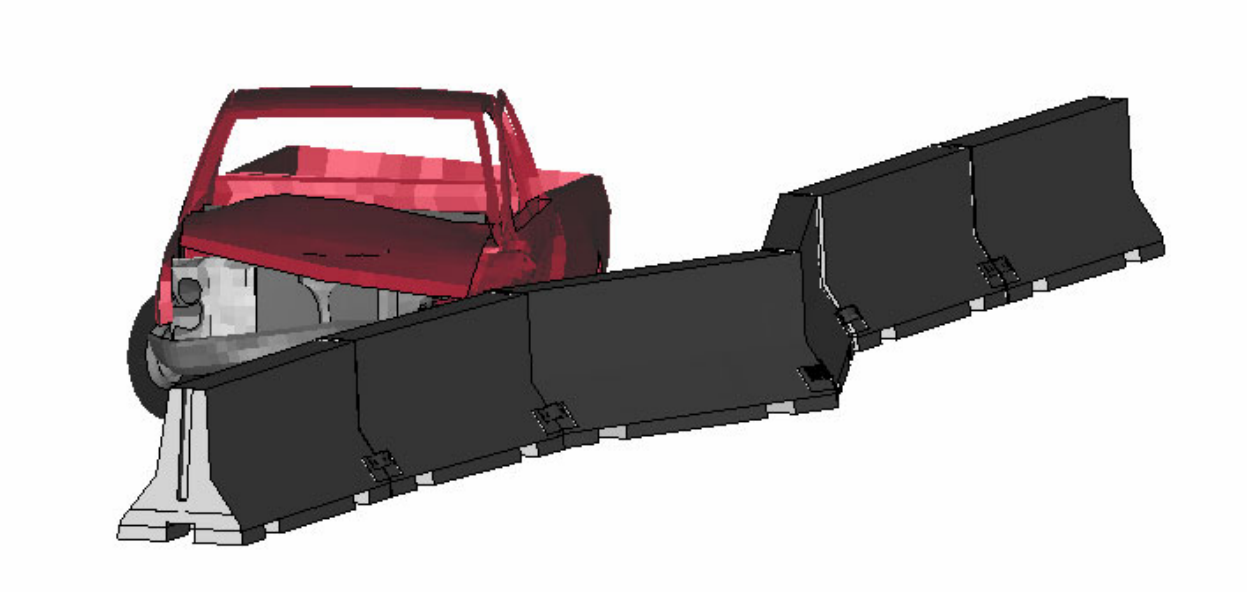

Figure 14. Simulated Grid-Slot PCB with Steel Straps After Impact.

Full-Scale Crash Test

The completed test installation consisted of eight barrier segments connected together for a total test installation length of approximately 240 ft (73 m). Photographs of the completed test installation are shown in Figure 15. Additional details of the test can be found in reference (*9*).

Figure 16 shows photographs of the damaged barrier after the test. The test vehicle was successfully contained and redirected, and the modified Texas grid-slot portable concrete barrier with steel straps and rebar grid met all required *NCHRP Report 350* evaluation criteria. The addition of 4-inch (102 mm) wide × 3/16-inch (5 mm) thick steel straps bolted to the face of the barrier segments across the joints substantially reduced the maximum dynamic deflection of the barrier. The maximum lateral barrier movement experienced in the test was 4 ft (1.2 m) under design impact conditions. Use of the steel strap connection will, therefore, permit the grid-slot barrier to be used in more restricted work zone areas.

In the crash test, one of the steel straps failed in tension on the field side of the barrier. It is logical to conclude that if the strength of the steel plate can be further increased to avoid failure of the strap without inducing failure of the anchor bolts that the barrier deflection can be further decreased. An additional series of computer simulations were conducted to investigate this issue. It was determined that if the size of the steel strap is increased to 6 inches (152 mm) wide × 1/4 inch (6 mm) thick, tensile failure of the strap can be avoided and barrier deflections should be reduced to approximately 3.25 ft (1.0 m). Images of the simulated barrier with modified steel straps after impact are shown in Figure 17. Besides the change in plate dimensions, all other details of the connection, including anchor bolt size and location, remain the same as those used in the crash test. Since this reduction in deflection can be achieved with only a small increase in material cost, it is recommended that the 6-inch (152 mm) wide × 1/4-inch (6 mm) thick steel straps be implemented when site conditions cannot accommodate large deflections and a retrofit connection alternative is warranted.

SUMMARY AND CONCLUSIONS

The crash performance of the TxDOT Type 2 precast concrete traffic barrier (PCTB[1]-90) with joint type A was unproven with respect to the *NCHRP Report 350* guidelines. Under this project and Research Project 0-4162, TTI researchers and TxDOT engineers worked together to evaluate the crash performance of this barrier and determine if cost effective modifications can be made to limit dynamic deflections to practical levels.

The design of the joint has a direct influence on the magnitude of lateral barrier deflection during a vehicular impact event. Various analyses were performed to help guide the barrier evaluation process and assess the ability of the selected barrier modifications to limit deflections prior to conducting the full-scale crash testing. Computer simulations of full-scale barrier impacts were performed using the LS-DYNA finite element code to help evaluate two different connection alternatives: a U-bar connector and steel straps.

Figure 15. Grid-Slot Barrier with Steel Strap Retrofit Before Crash Test.

Figure 16. Grid-Slot Barrier with Steel Strap Retrofit After Crash Test.

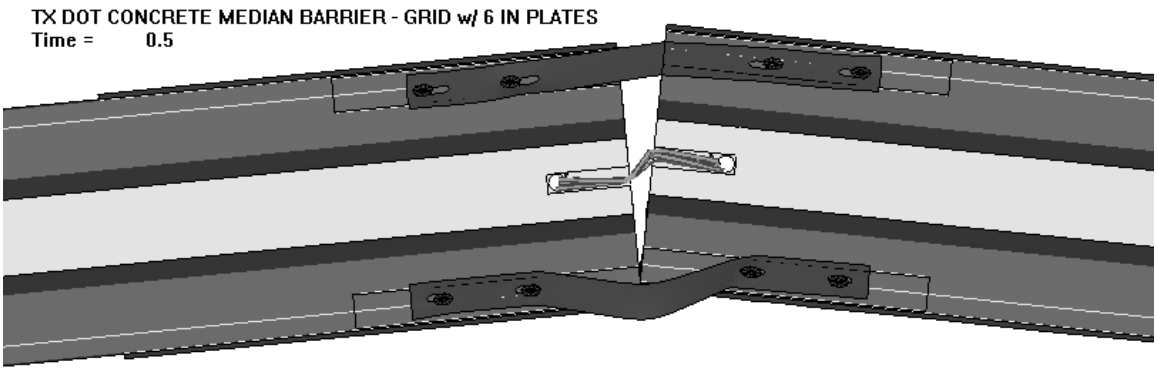

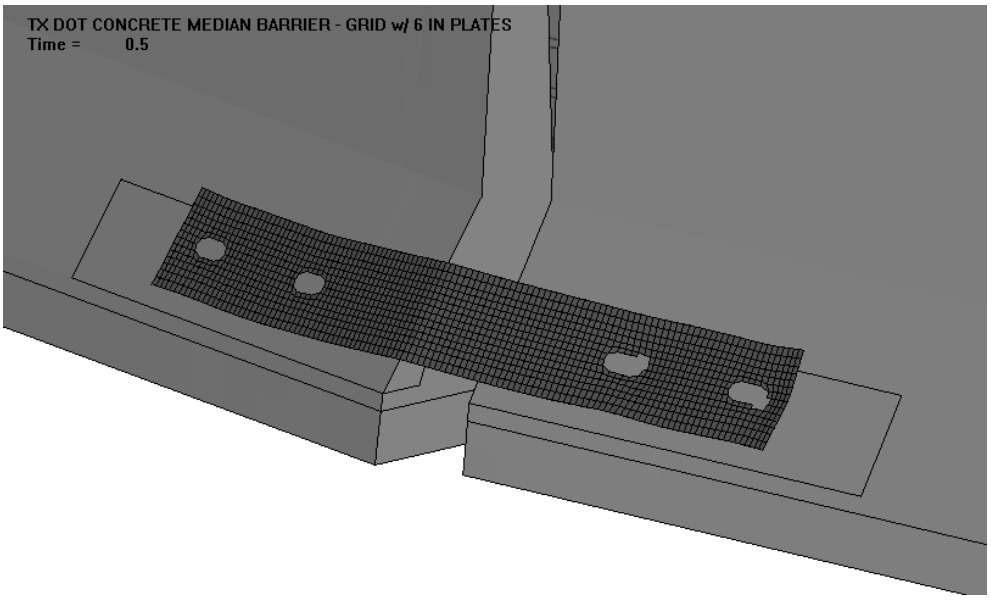

Figure 17. Simulated Grid-Slot Barrier with Modified Steel Strap After Impact.

Subsequent to the simulation work, crash tests were performed under Research Project 0-4162 in the order of the cost-effectiveness of the retrofit barrier modifications. The purpose of the tests was to quantify any relative improvements in crash performance and lateral barrier deflection.

Although each retrofit barrier configuration met *NCHRP Report 350* guidelines, variations in performance associated with the different connection details were observed. The tensile capacity of the U-bar connector was limited by the shear strength of an unreinforced section of concrete beneath the slots precast into the barrier ends to accept the rebar grid. After failure of this concrete block, the integrity of the connection immediately downstream of the point of impact was lost and the unconstrained barrier ends deflected 12.4 ft (3.8 m).

Comparatively, the steel strap limited the barrier deflection to 4 ft (1.2 m). Although one of the straps ruptured in tension on the field side of the barrier, the failure did not occur until after the vehicle had passed the joint and a considerable reduction in deflection was realized. Subsequent analyses indicated that if the size of the steel straps is increased from 4 inches (102 mm) × 3/16 inch (5 mm) to 6 inch (152 mm) × 1/4 inch (6 mm), rupture of the plate should be avoided and the barrier deflection would decrease to approximately 3.25 ft (1.0 m).

The reduced deflection offered by the steel strap retrofit connection comes with an increase in installation cost and labor. The connection requires four holes to be drilled into each end of the barrier segments to accommodate the anchor bolts that secure the steel strap to the toe of the barrier segment. The bolting operation, which requires eight anchor bolts at each joint, is more time-consuming than a drop-in connector and will thus increase exposure of work zone personnel.

CHAPTER 4. DEVELOPMENT OF GUIDELINES FOR PLACEMENT OF MOW STRIPS AROUND GUARD FENCE

BACKGROUND

An area of particular interest and concern to TxDOT is the performance of guard fence encased within a mow strip. Standard strong post guard fence systems comprised of W-beam rail mounted on either W6×9 (W150×14) steel or 7-inch (178 mm) diameter round wood posts have been in use for many years and have performed well. Recent environmental concerns related to the use of herbicides for control of roadside vegetation, and increased efforts to reduce hand mowing around guardrails posts for both safety and cost reasons, has led many districts to adopt the practice of encasing guard fence posts in either a concrete or asphalt mow strip. Since there is no statewide standard, each district addresses the practice differently. Current practice varies from entirely encasing the perimeter of the guardrail post within the mow strip to providing a small "cutout" around the post to permit some degree of rotation or lateral deflection.

These mow strips appear to be cost-effective for vegetation control in terms of reducing the exposure of workers and cost of routine maintenance at these locations. However, the vehicle safety risk associated with this practice has not been evaluated. There is concern that, if not properly designed, these mow strips may negatively influence the impact performance of guard fence by promoting premature failure of the guard fence posts and/or increased vehicle snagging during a crash event.

The degree of soil confinement and post fixity created by the mow strip varies with the design details. Depending on the design, the post rotation will be restricted or altogether prevented. Thus, the force-deflection characteristics and energy absorption capability of the posts can be significantly altered. Premature failure/fracture of wood posts can lead to pocketing of the vehicle and tensile rupture of the guardrail element. The constrained rotation of steel posts can promote increased wheel snagging, which in turn can result in high decelerations and/or instability of the impacting vehicle. The mow strips may also adversely influence safety by making the repair of guardrail installations more difficult and time-consuming after they have been struck.

RESEARCH OBJECTIVES/SCOPE

The primary objective of this research was to develop recommended practices for installing guardrail in mow strips from which a standard can be developed. These improved practices are intended to reduce the potential for injury to motor vehicle occupants involved in run-off-road crashes and reduce the time, cost, and exposure associated with maintenance and repair operations.

Due to the lack of standards associated with this widespread practice, there is no uniformity in design throughout Texas. Variables include the mow strip material and thickness, the existence and size of leave-outs, the type of guard fence post, and the type of fill material

used in the leave-out (if one exists). Since the variables are not bounded by a standard and it would be impractical from a cost standpoint to conduct a parametric investigation based solely on crash testing, the problem lends itself to initial analysis and evaluation through computer simulation. The research approach involved a combined program of component testing, computer simulation, and full-scale crash testing to evaluate the effect of mow strips on the performance of guard fence.

TxDOT and FHWA jointly funded the computer modeling and simulation portions of this research. This joint funding maximized the available resources and enabled the research team to fully investigate and develop useful and practical guidelines for guard fence encased in mow strips. The component and full-scale testing portions of this research were supported under Research Project 0-4162 (*10*). Details of the mow strip analyses are described below.

COMPONENT EVALUATION

The ranges of design parameters considered under this research effort were selected based on the results of a district-level survey and input received from the TxDOT project advisory panel. Design variables that were considered include mow strip material type, mow strip thickness, size and shape of leave-outs, type of backfill material used in the leave-outs, and type of guard fence post.

Given the large number of design variables and treatment options that exist for this practice, full-scale crash testing of the entire matrix would be cost-prohibitive. Rather, a subcomponent-level investigation was performed to develop a better understanding of the response of mow strip systems subjected to dynamic impact loads. The subcomponent evaluation phase consisted of both dynamic impact testing with a "bogie" vehicle and finite element simulation. The test matrix, shown in Table 3, incorporates several key design variables that relate to common TxDOT practices and are deemed most critical to mow strip performance.

Following the prescribed test matrix, the dynamic response of steel and wood guard fence posts confined in various mow strip treatments was evaluated using a surrogate bogie test vehicle with a crushable honeycomb nose calibrated to approximate the frontal crush stiffness of a small passenger car. The bogie vehicle impacted each post head-on at a speed of 21.7 mph (35 km/hr). Load-deflection response, energy absorption characteristics, and the failure mode of the posts in different mow strip treatments with and without leave-outs were compared with the results of similar tests on conventional soil-embedded guard fence posts. The test results provided an objective basis for determining which treatments offered potential for meeting crash test requirements. The data were also used to assist in the development and validation of component and subsystem models for use in predictive full-scale computer simulations.

Table 3. Test Matrix of Mow Strip Configurations.

Case (1)	Mow Strip Material (2)	Post Type (3)	Leave-Out Material (4)	Leave-Out Size (5)	Leave-Out Depth (6)
1	None	Wood	N/A	N/A	N/A
2	None	Steel	N/A	N/A	N/A
3	Asphalt	Wood	Asphalt	305 mm Dia.	200 mm
4	Asphalt	Wood	Asphalt	457 mm Dia.	200 mm
5	Asphalt	Steel	Asphalt	305 mm Dia.	200 mm
6	Asphalt	Steel	Asphalt	457 mm Dia.	200 mm
7	Concrete	Wood	N/A	N/A	N/A
8	Concrete	Wood	Grout	457x457 mm	100 mm
9	Concrete	Wood	Grout	457x607 mm	100 mm
10	Concrete	Steel	N/A	N/A	N/A
11	Concrete	Steel	Grout	457x457 mm	100 mm
12	Concrete	Steel	Grout	457x607 mm	100 mm
13	Asphalt	Wood	Grout	457 mm Dia.	100 mm
14	Asphalt	Steel	Grout	457 mm Dia.	100 mm
15	Asphalt	Wood	Asphalt	457 mm Dia.	100 mm
16	Asphalt	Steel	Asphalt	457 mm Dia.	100 mm
17	Asphalt	Steel	Rubber Mat	457 mm Dia.	N/A

An asphalt mow strip was constructed by placing PG64-22 hot mix asphalt with Type D aggregate over a 1 ft (0.3 m) thick layer of compacted base material. The mow strip was 8 inches (203 mm) thick and 3.5 ft (1.07 m) wide. Using a mechanical roller, the asphalt was compacted to approximately 90 percent of the lab density. The in-place density of the asphalt was measured to be 151.4 lb/ft^3 (2425 kg/m^3) using a nuclear densometer. Holes were augered through the asphalt for placement of the wood and steel guardrail post. The 7-inch (178 mm) diameter wood and W6×9 (W150×14) steel guard fence posts were set in the holes to a depth of 3.75 ft (1.1 m). The void area around the post was backfilled with standard *NCHRP Report 350* soil to within several inches of the surface of the mow strip. Both two-sack grout and hand-tamped hot mix asphalt were selected for use in the upper portion of the leave-outs around the posts. Alternative leave-out materials such as foam and recycled rubber mats were also considered. The construction of the asphalt mow strip test installation is shown in Figure 18.

The concrete mow strip was constructed using TxDOT Class B riprap concrete with a minimum 28-day compressive strength of 2031 psi (14 MPa). The concrete was reinforced throughout with welded-wire mesh reinforcement with the exception of the leave-out sections formed around the posts. The mow strip was 5 inches (127 mm) thick, 3.5 ft (1.07 m) wide, and 43.8 ft (13.3 m) long. The posts were embedded in augured holes to a depth of 3.6 ft (1.1 m) and backfilled with *NCHRP Report 350* standard soil. Due to its low cost, ease of installation, overall effectiveness, and matching appearance, a two-sack grout mixture was used as the backfill material in the top 4 inches (102 mm) of the leave-outs. As a baseline, one wood post and one steel post were directly encased in the concrete mow strip without a leave-out section. The constructed concrete mow strip test installation is shown in Figure 19.

Figure 18. Asphalt Mow Strip Installation Used for Dynamic Impact Tests.

Figure 19. Concrete Mow Strip Installation Used for Dynamic Impact Tests.

To understand the effect of encasing guardrail posts in mow strips, it is necessary to have a point of reference from which to compare changes in performance. Both the modified G4(1S) steel post guardrail system and round wood post guardrail system have met *NCHRP Report 350* criteria with standard soil embedment. To compare performance of posts encased in mow strips to post configurations that have demonstrated successful performance in crash tests, standard soil embedment was used as the baseline test configuration for each post type.

Seventeen dynamic impact tests were performed on a series of mow strip configurations following the matrix shown in Table 3. As expected, direct concrete confinement of the posts represented a severe impact scenario. The bogie impact caused severe damage to the concrete mow strip around the steel post with little movement of the post (see Figure 20 [a]). By contrast, the wood post fractured rapidly upon impact, thereby reducing damage to the concrete mow strip, but permitting the bogie vehicle to pass through relatively unimpeded (see Figure 20 [b]). In both cases, the concrete mow strip allowed minimal deflection of the post at the groundline and created a costly repair situation.

(a) Steel Post in Concrete

(b) Wood Post in Concrete

(c) Steel Post in Grout-Filled Leave-Out

(d)Wood Post in Grout-Filled Leave-Out

Figure 20. Posts in Concrete Mow Strip After Impact.

At thicknesses of 4 inches (102 mm), the hand-tamped hot-mix asphalt leave-out material did not allow either wood or steel posts to deflect. The wood posts fractured at the groundline and the steel posts twisted and yielded without significant translation. The presence of a leave-out with grout backfill material greatly improved impact performance of the posts in both the concrete and asphalt mow strips. As shown in Figure 20 (c) and Figure 20 (d) for the steel post and wood post, respectively, the grout broke up as the posts were impacted, allowing them to deflect to the back of the leave-out section prior to yielding or fracturing. This added post deflection offers to greatly improve the performance of a full-scale guardrail system.

NUMERICAL SIMULATION OF COMPONENTS

By testing single post installations in the manner described above, the behavior of individual guardrail system components such as the posts, soil, and leave-out backfill material can be studied. As a first step in modeling full-scale guardrail installations encased in a mow strip, finite element models of these components were developed. Component modeling allows the researchers to gain confidence in the accuracy of smaller-scale models before assembling the full system model and using it in predictive simulations. Posts, soil, mow strip confining layers, W-beam guardrail segments, and other components comprising the guardrail system were studied using subcomponent finite element models. Results from numerical simulations of these models were compared with the results of the bogie impact tests to validate accuracy of the models.

A finite element model of the Federal Outdoor Impact Laboratory (FOIL) bogie impactor was obtained for use in simulating the experimental bogie vehicle tests *(11)*. The model consists of 1,844 elements and 2,985 nodes. The frame of the vehicle is modeled using both rigid and linearly elastic beam elements. The metallic honeycomb cartridges are modeled with an anisotropic, nonlinear, elastoplastic material model for honeycomb and foam materials.

To calibrate the bogie vehicle model with the TTI bogie vehicle, an impact test of the TTI bogie vehicle into an instrumented rigid pole was simulated. Researchers noted that the frame of the TTI bogie vehicle includes a flexible suspension not included in the FOIL bogie or the FOIL bogie model. Consequently, the TTI bogie absorbs energy through elastic deformation of the flexible suspension. It, thus, became necessary to modify the numerical model to account for the elastic suspension in the TTI bogie. With the addition of springs and dampers, response of the bogie model more closely follows the test data. An acceleration history for the modified FOIL bogie (or TTI bogie) is shown in Figure 21.

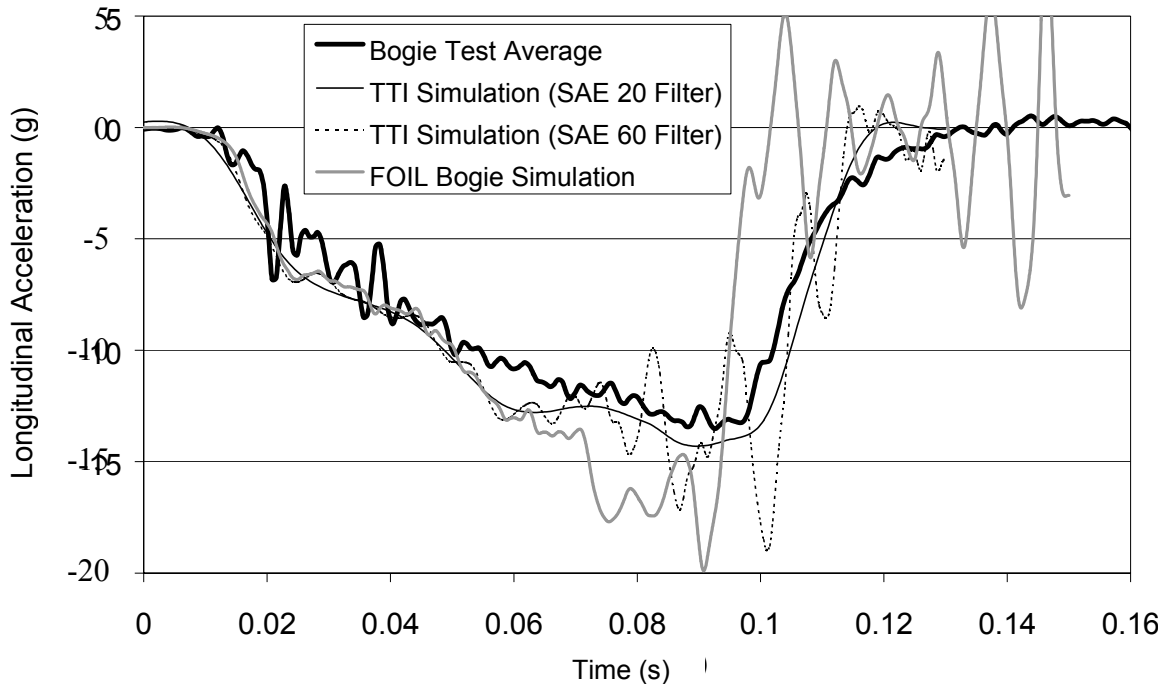

Figure 21. Accelerations of Bogie for Simulation Calibration.

Several material models are available in LS-DYNA to represent soil. In order to capture the increase in shear strength under normal stress demonstrated by cohesionless soils, the model proposed by Drucker and Prager was used in this study *(12)*. Drucker and Prager proposed a modification of the Mohr-Coulomb criterion to take into account the inability of a cohesionless soil to resist tensile loading *(12)*. The result of this modification was a soil with increased shear strength under normal stress. With the shearing deformation comes volumetric expansion. By comparing the results of the simulation to the corresponding bogie tests, the input properties to the soil material model were calibrated within published ranges for the *NCHRP Report 350* standard soil.

The isotropic, elastoplastic behavior of steel is considerably more straightforward to represent in a numerical model than the anisotropic, nonlinear behavior of wood. In addition, the failure mechanisms of steel guardrail posts, including yielding and buckling, are more reliably modeled than fracture and splitting of wood. The steel posts were numerically modeled using a piecewise linear plasticity material model. Before yield, the material is assumed to be linearly elastic. After yielding, the steel can undergo plastic deformation and strain hardening. The required material properties were obtained from a series of three tensile tests on steel coupons taken from guardrail posts*(13)*.

Using numerical models of a steel post and soil, the conditions of the dynamic impact test with the steel post embedded in soil were replicated. Figure 22 shows the initial configuration for the numerical simulation. Sequential images of the numerical simulation and experimental testing are shown in Figure 23. Impact of the bogie vehicle causes the steel post to deflect

through the soil. The soil response, post deflection, and post deformation are consistent between the experimental test and simulation.

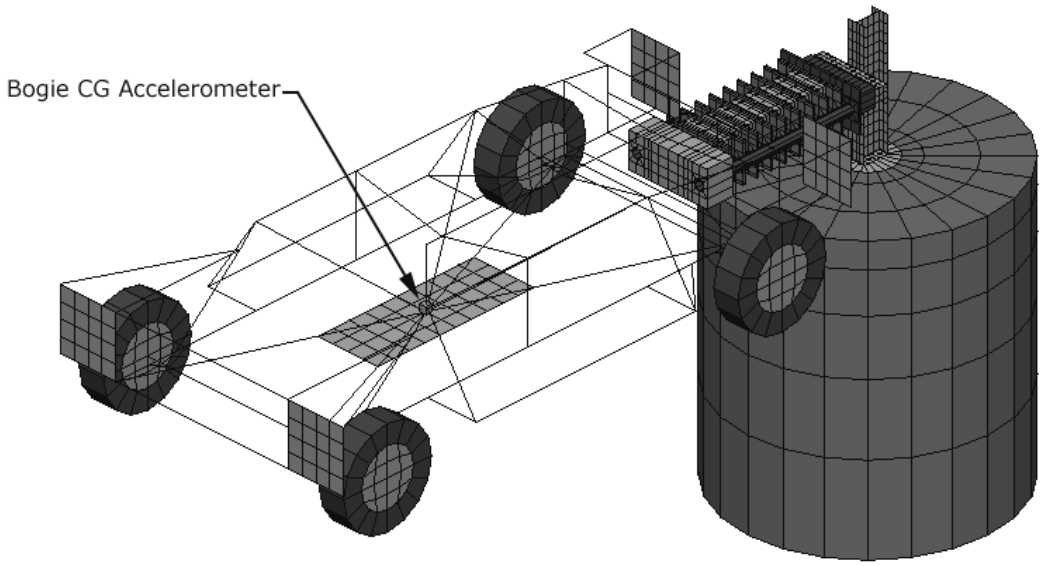

Figure 22. Initial Configuration of Steel Post Baseline Bogie Simulation.

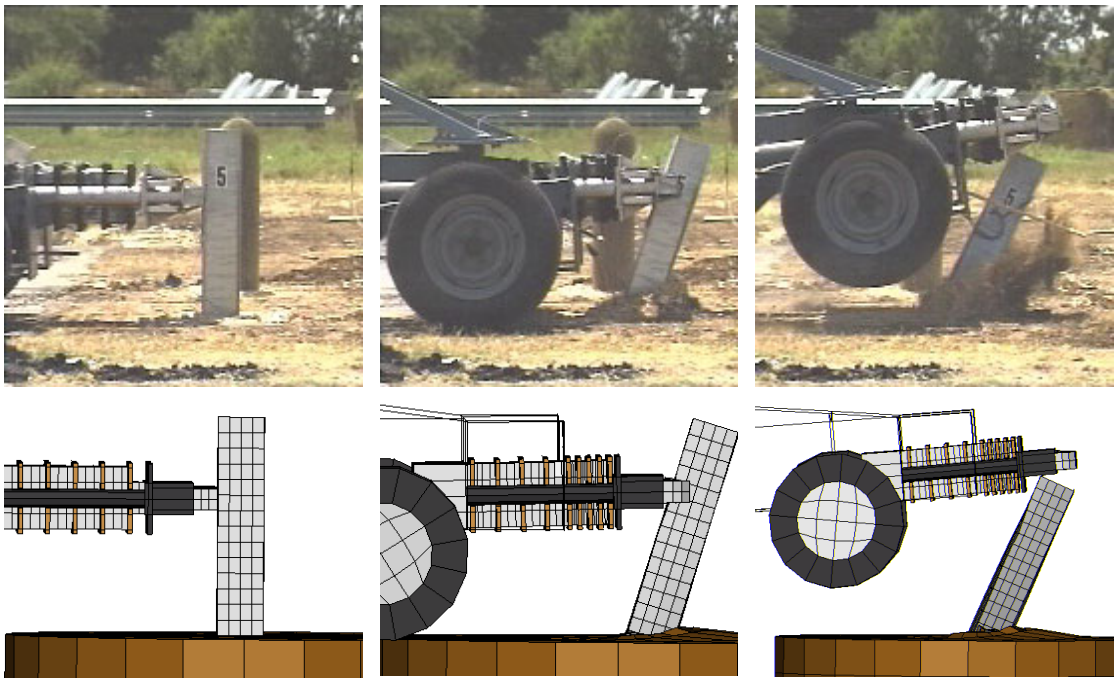

Figure 23. Sequential Comparison of Test and Simulation for Steel Post in Soil.

Figure 24 shows a comparison of longitudinal accelerations of the bogie for the experimental test and numerical simulation (both filtered using an SAE 180 Hz filter). Results of numerical simulation follow the same trend as the experimental test data. After the peak acceleration is reached, the numerical simulation demonstrates high-frequency oscillation. This oscillation is induced by the springs added to the bogie model to account for the behavior of the suspension system.

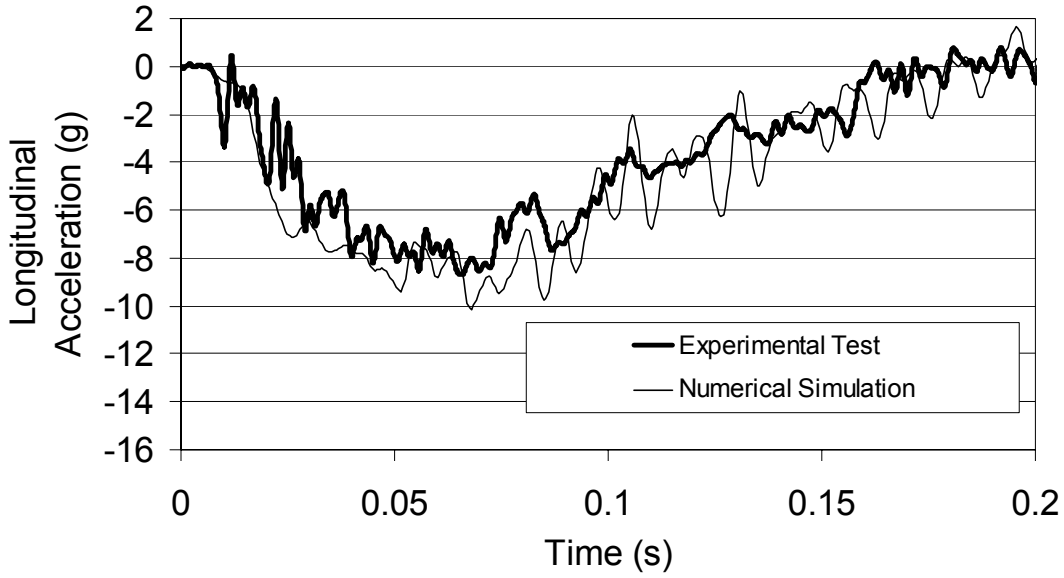

Figure 24. Simulation and Test Accelerations of Bogie for Steel Post in Soil.

Wood is a complex material with different mechanical properties along the grain and perpendicular to the grain. Several LS-DYNA material models were examined to represent the behavior of wood. While testing some of the more complex material models (e.g., material 59) to model the behavior of a wood post, several numerical instabilities were encountered. Ultimately, material 13, *Isotropic Elastic Failure*, with a strain based failure criterion was used in this project. The required material properties for this model were calibrated using the bogie test data. As with the steel post simulation, good correlation of soil response, post deflection, and bogie acceleration was achieved between the experimental test and simulation of the wood post in soil.

Additionally, in order to be able to assess the effects of mow strip confinement on post response, it was necessary for the wood post model to accurately capture failure/fracture under confined conditions. Therefore, to complete the validation of the wood post model, a simulation of the bogie test of a wood post in asphalt mow strip was performed. The asphalt mow strip impact test was selected to avoid the complications of concrete fracture that occurred during the concrete mow strip tests. In the asphalt mow strip test, the post fractured with minimal displacement.

Sequential images of the numerical simulation and experimental test are shown in Figure 25. In each case, impact of the bogie vehicle caused the wood post to fracture. The post

failure pattern is consistent between the experimental test and simulation. Based on these results, the wood post model was considered sufficiently valid for use in full-scale system models.

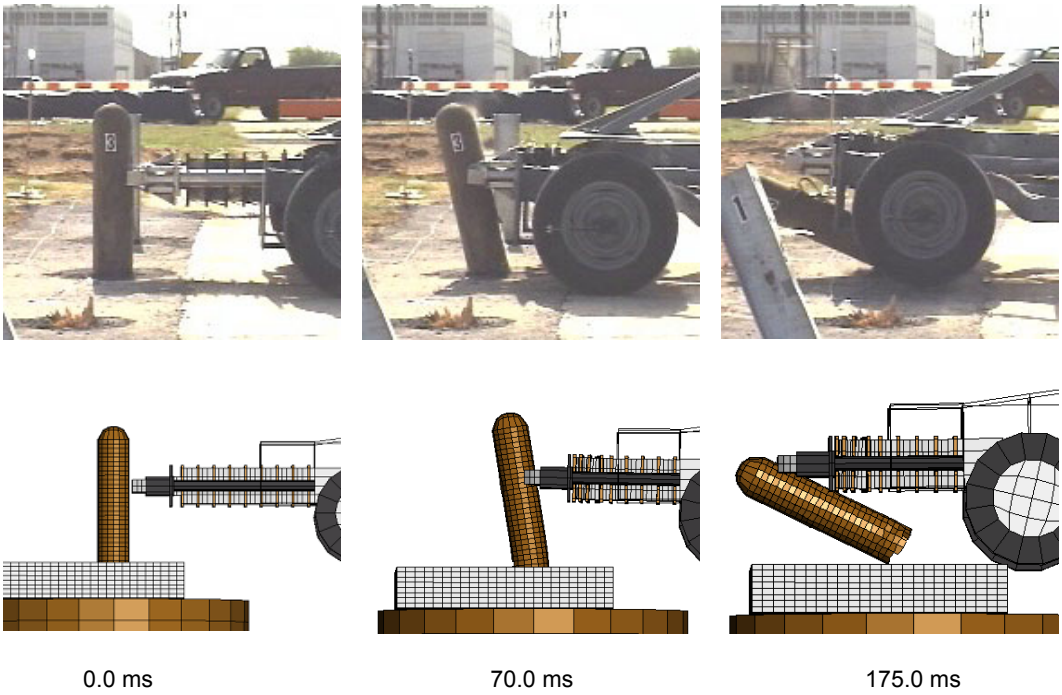

Figure 25. Sequential Comparison of Simulation and Test Results for Wood Post in Asphalt.

The grout material used as backfill in the upper region of the leave-outs was modeled using material 13, *Isotropic Elastic Failure*. This material model allows the user to specify a failure pressure for element erosion. When the pressure in an element reaches a specified failure value, the element is eroded. The failure pressure for the grout material model was calibrated using results of a bogie impact simulation of a steel post in asphalt mow strip with an 18-inch (457 mm) diameter grout-filled leave-out (see Figure 26). The asphalt mow strip impact test was used for validation to avoid the complications of concrete fracture that occurred during the concrete mow strip tests.

Figure 27 shows slight variation between the bogie accelerations obtained from the experimental test and simulation. However, there is reasonable correlation of both the maximum acceleration and the rate of change of acceleration. Future simulations can improve the grout model by implementing a more sophisticated failure criterion; however, by modeling the peak capacity of the grout before failure, an accurate representation of post deflection can be achieved with this grout model.

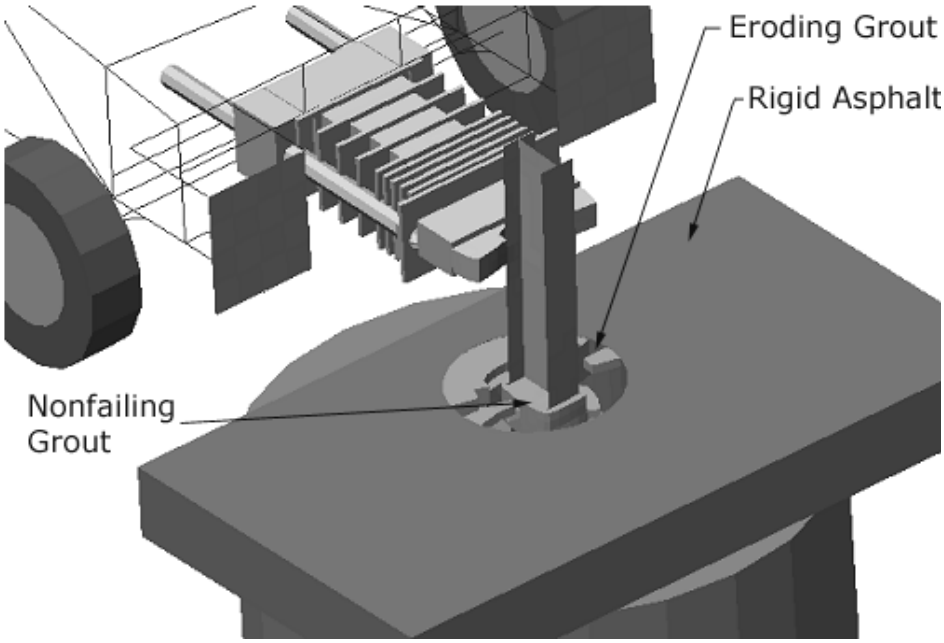

Figure 26. Bogie Impacting Steel Post Surrounded by Eroding Grout Elements.

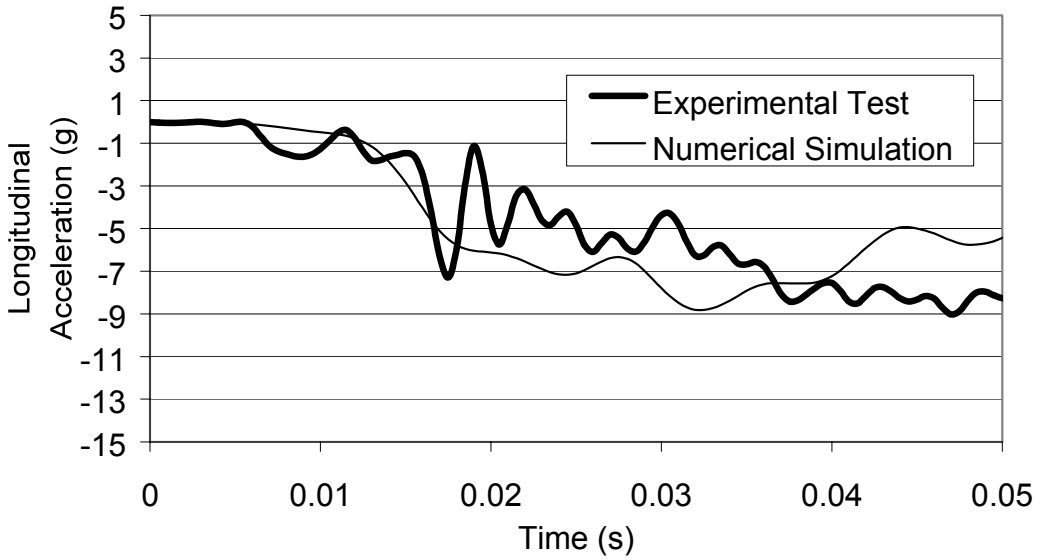

Figure 27. Simulation and Test Accelerations of Bogie for Steel Post in Grout-Filled Leave-Out.

PREDICTIVE FULL-SCALE SYSTEM SIMULATIONS

Using the component models described above, full-scale finite element models for several different guardrail configurations were developed. A full-scale finite element model of a modified G4 (1S) steel post guardrail system was developed and used in impact simulations as a reference benchmark for the mow strip configurations and as a mean of validating the system models. The full system, which is 100 ft (30 m) long, consists of 90,573 elements and 108,782 nodes, not including the vehicle model.

The simulation followed the impact conditions of *NCHRP Report 350* Test 3-11, which involves a 4405-lb (2000 kg) pickup truck impacting the guardrail at a speed of 62 mph (100 km/h) and an angle of 25 degrees. The numerical simulation showed the test vehicle being smoothly redirected without severe snagging or pocketing and exiting the system in a stable manner without considerable roll (see Figure 28). Maximum dynamic guardrail deflection, overall vehicle dynamics, and vehicle damage were consistent between test and simulation.

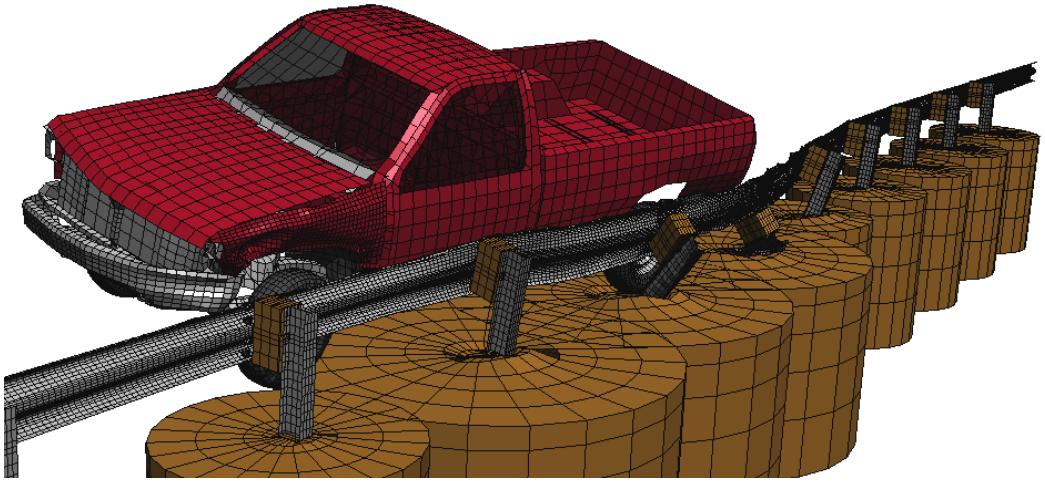

Figure 28. Vehicle Impacting Modified G4(1S) Steel Post Guardrail System.

With numerical simulation of the G4 (1S) guardrail system demonstrating behavior that is typical of full-scale crash tests, this numerical model was used as a baseline model to construct other finite element models of mow strip guardrail system variations. Four numerical models of mow strip guardrail configurations were developed for use in predictive simulations to assess their ability to meet *NCHRP Report 350* criteria. These include wood and steel post guardrail encased in a rigid concrete mow strip, and wood and steel post guardrail encased in a concrete mow strip with grout-filled leave-outs around the posts.

Guardrail Encased in Rigid Mow Strip

To investigate the effect of having a guardrail system completely encased in a concrete or asphalt mow strip without leave-outs around the posts, finite element models for steel post and

wood post guardrail systems encased in a rigid mow strip were constructed. The mow strip was assumed rigid to represent a worst-case scenario in regard to pavement-post confinement in which no movement (rotation) of the post is allowed. This assumption is realistic since relatively thick concrete and asphalt mow strips are used in practice.

As expected, the rigid concrete mow strip system produces a severe impact response. As shown in Figure 29, the rigid mow strip restricts the bases of the steel posts from deflecting. The severe post snagging that ensues destabilizes the vehicle, causing it to climb above the top of the rail. The lack of post rotation also causes increased stresses in the W-beam rail and increased deformation of the lower edge of the rail. The plastic strain contours in the rail, which are in excess of 30 percent over substantial portions of the rail, indicate a high probability of rail rupture. In summary, the results indicate that a steel post guardrail directly encased in a rigid mow strip has a low probability of passing *NCHRP Report 350* evaluation criteria.

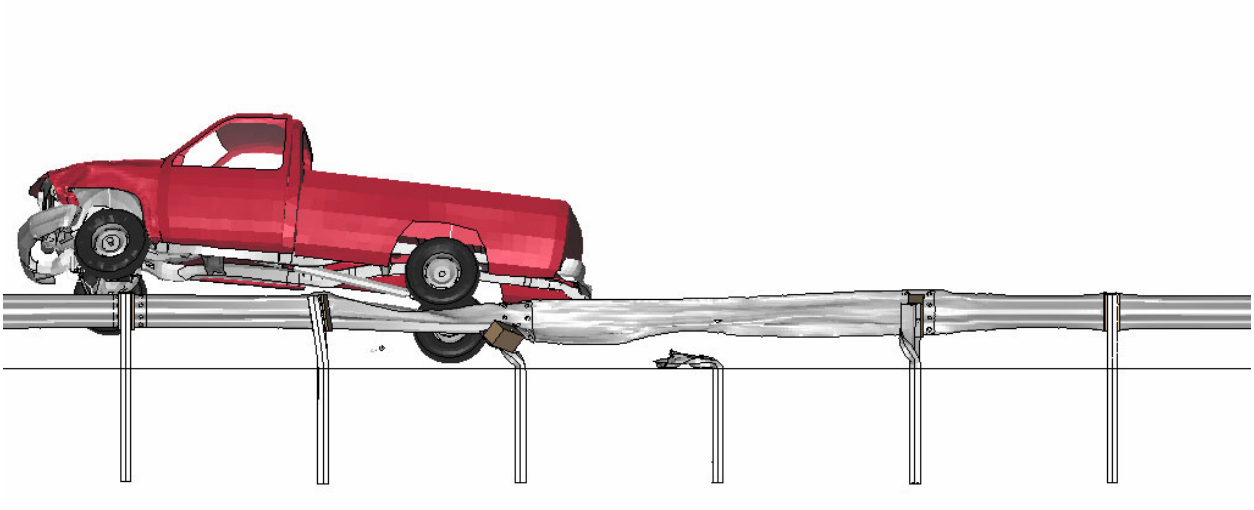

Figure 29. Vehicle Instability During Impact of Steel Post Guardrail in Rigid Mow Strip.

To investigate the impact performance of a wood post guardrail completely encased in concrete or asphalt, a finite element model of a full-scale wood post guardrail system encased in a rigid mow strip was constructed. The model was similar in detail to the previously described steel post guardrail system but with the validated wood post model substituted for the steel posts. Again, the mow strip is assumed rigid to represent the critical case where no movement (rotation) of the post is allowed.

The constraint imposed by the rigid mow strip caused four wood posts to fracture during the impact. Because the posts fractured in advance of the vehicle, there was no snagging contact between the vehicle and the posts and, therefore, the vehicle remained relatively stable. However, the loss of four posts did produce some pocketing of the vehicle in the rail system as evident in Figure 30. This pocketing behavior led to some kinking and high plastic strains along a cross section of the rail located at the post at the downstream end of the pocket. These strains indicate a high probability of W-beam rupture at this post, particularly if it happens to coincide with a rail splice location. In summary, the results indicate that this system has a low probability of passing *NCHRP Report 350* evaluation criteria.

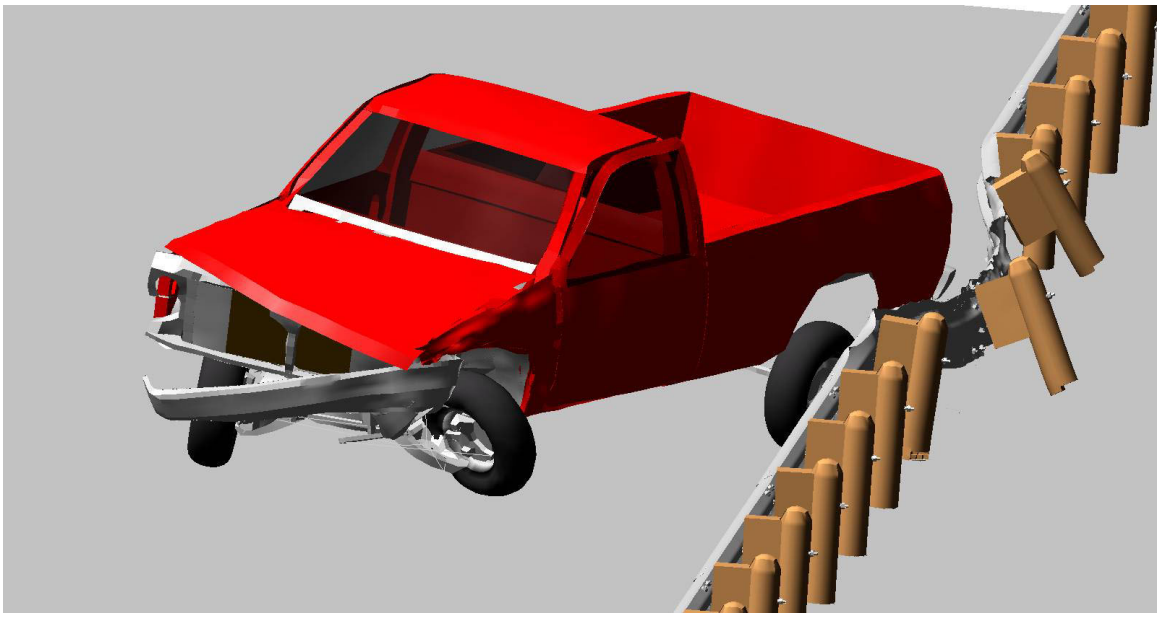

Figure 30. Vehicle Pocketing During Impact of Wood Post System in Rigid Mow Strip.

Guardrail in Concrete Mow Strip with Grout-Filled Leave-Outs

A finite element model of a steel post guardrail encased in concrete mow strip with grout-filled leave-outs was modeled and used in a predictive crash simulation to assess the ability of the system to meet *NCHRP Report 350* performance requirements (see Figure 31). The dimensions of the leave-outs were 18 inches × 18 inches (457 mm × 457 mm). The top 4 inches (102 mm) of the leave-out was backfilled with two-sack grout. The traffic face of the steel guardrail posts were offset 3 inches (75 mm) from the front edge of the leave-out.

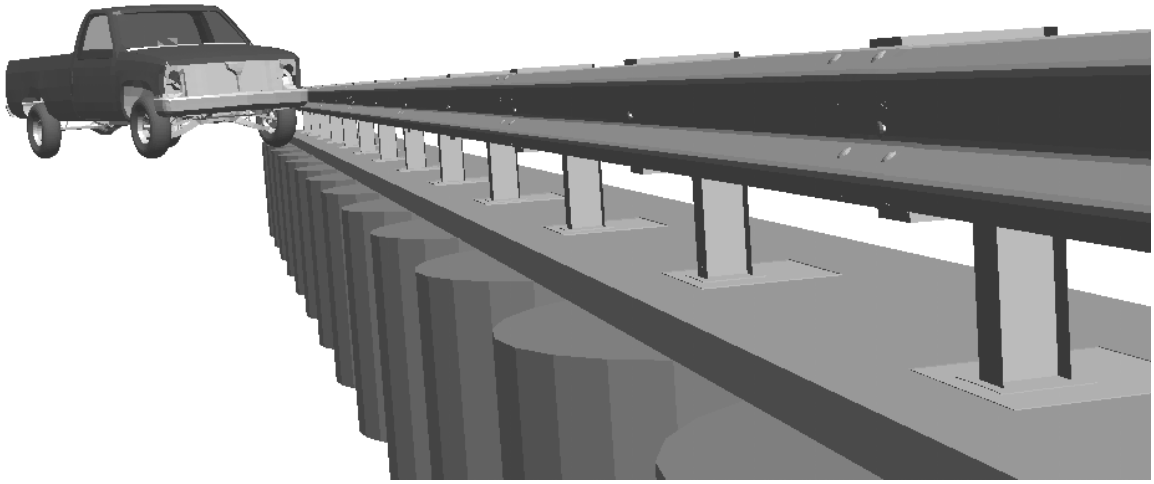

Figure 31. Initial Configuration for Steel Post Guardrail System in Concrete Mow Strip with Grout-Filled Leave-Outs.

The steel posts were able to rotate and deflect within the mow strip due to the failure of the weak grout backfill material inside the leave-outs. The post movement mitigated the severe vehicle-post snagging observed in the rigid mow strip simulation. Consequently, the vehicle was redirected in a much smoother manner without significant climb or roll. Two posts disengaged from the rail and some were deflected and twisted in a manner reminiscent of soil-embedded steel posts. Plastic strain contours of the rail indicate localized concentrations of high strain around bolts slots and moderate plastic strain throughout the remainder of the rail segment. This indicates that rupture in the rail segment is not probable and only a few small tears around the slots are likely to develop.

In summary, the numerical simulation shows that the grout-filled leave-outs provide significant improvement in impact performance over direct concrete embedment. The post snagging is still more severe than that observed for the soil-embedded system, but the vehicle is much more stable and the rail stresses and strains are within acceptable levels. The steel post guardrail system encased in concrete mow strip with grout-filled leave-outs is considered to have a high probability of passing *NCHRP Report 350* criteria and was recommended for full-scale crash testing.

To investigate the *NCHRP Report 350* compliance of a wood post guardrail system encased in concrete mow strip with grout-filled leave-outs, researchers constructed a full-scale finite element model of the system. The model was similar in detail to the steel post guardrail system with grout-filled leave-outs, but with the validated wood post model substituted for the steel posts.

As shown in Figure 32, the wood posts were able to rotate and deflect within the mow strip due to the failure of the weak grout backfill material inside the leave-outs. Compared to the wood post system in rigid mow strip, the number of fractured wood posts was reduced from four to two. Further, these two posts fractured on the back edge of their leave-outs after dissipating a significant amount of energy by rotating through the soil. Consequently, the pocketing pattern did not develop in the rail, and the vehicle was redirected in a relatively smooth and stable manner. Plastic strain contours in the rail indicated localized concentrations of high strain around bolts slots and moderate plastic strain throughout the rail segment. This indicates that rupture in the rail segment is not likely and only a few tears around the slots are likely to develop. The wood post guardrail system encased in concrete mow strip with grout-filled leave-outs is considered to have a high probability of passing *NCHRP Report 350* criteria and was recommended for full-scale crash testing.

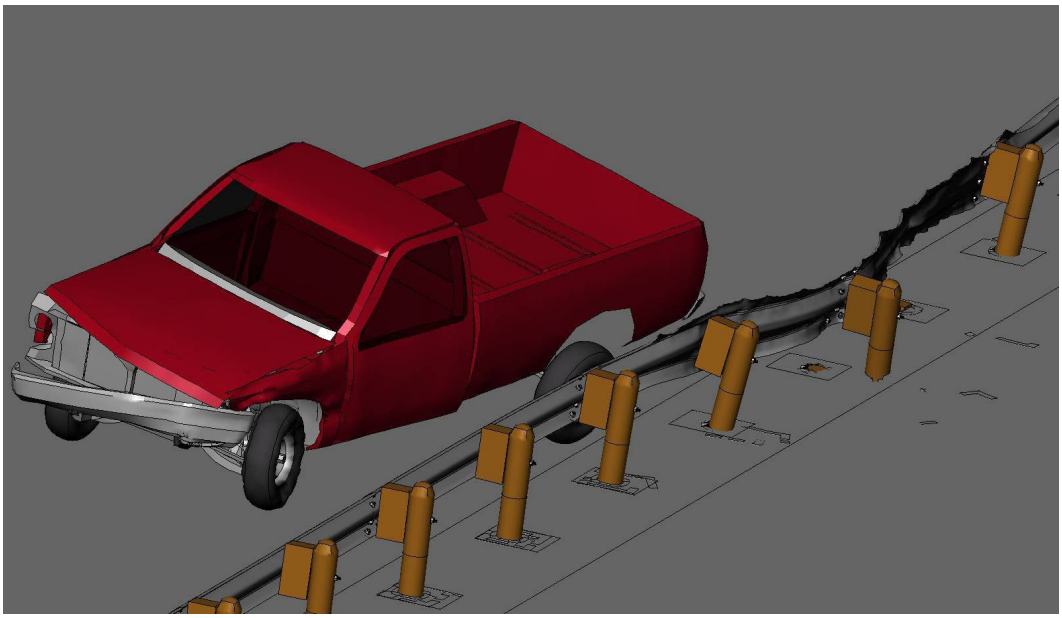

Figure 32. Vehicle Exiting Wood Post Guardrail System in Concrete Mow Strip with Grout-Filled Leave-Outs.

FULL-SCALE CRASH TESTING

Based on the results of the predictive impact simulations, two mow strip configurations were selected for full-scale crash testing to verify their compliance with *NCHRP Report 350*: a strong steel post W-beam guardrail and strong wood post W-beam guardrail encased in a concrete mow strip with grout-filled leave-outs around the posts.

The first crash test was performed on a W-beam guardrail mounted on W6×9 (W150×14) steel posts that were encased in a concrete mow strip with grout-filled leave-outs. The concrete mow strip constructed for the crash tests was 3 ft-6 inches (1.1 m) wide and 5 inches (127 mm) thick. It was constructed using TxDOT Class B riprap concrete with a minimum 28-day compressive strength of 2031 psi (14 MPa). To help avoid shrinkage cracking and separation of the mow strip from the adjacent test apron, a single layer of W6×W6 welded wire fabric was used to reinforce the concrete mow strip. An 18 inch × 18 inch (457 mm ×457 mm) leave-out section was formed around the guardrail posts. The traffic face of the posts was offset 3 inches from the front edge of the leave-out. The posts were set inside 18-inch (457 mm) diameter augered holes to a depth of 3.75 ft (1.1 m). The void area around each post was backfilled to within 4 inches (102 mm) of the top of the mow strip with *NCHRP Report 350* standard soil. The top 4 inches (102 mm) of the leave-out was backfilled with a two-sack grout mixture with a 28-day compressive strength of approximately 120 psi (0.85 MPa). Details of the steel post guardrail test installation are shown in Figure 33. Figure 34 shows a photograph of the completed test installation.

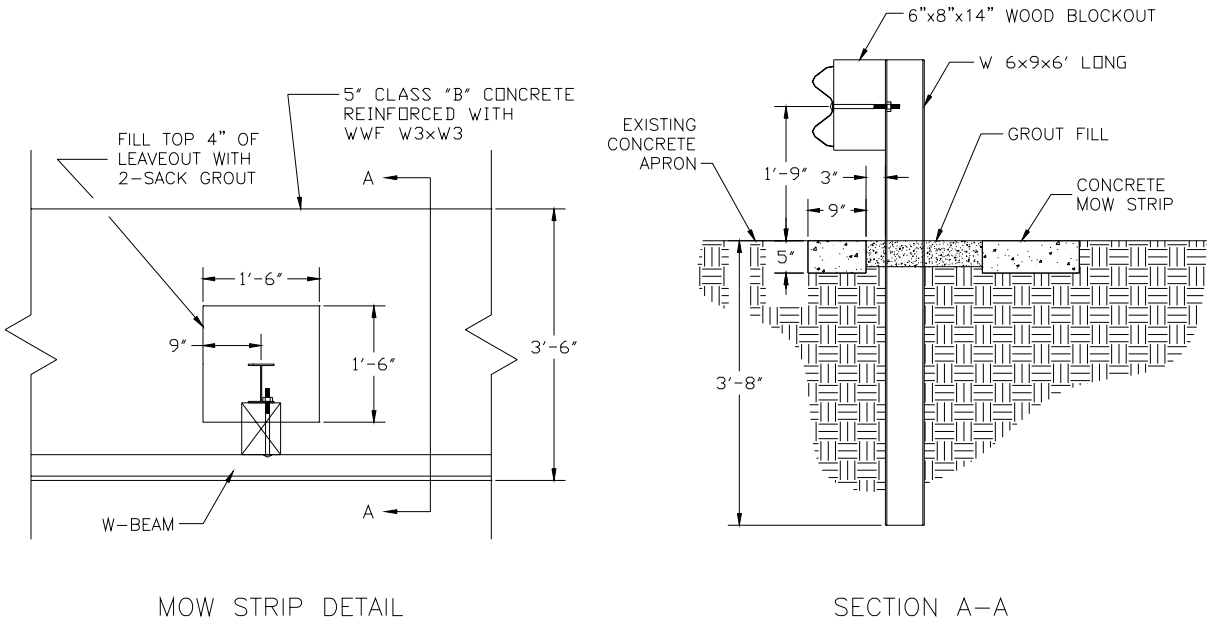

Figure 33. Details of Steel Post Guardrail Test Installation.

Figure 34. Completed Steel Post Guardrail Test Installation.

For the second test, a similar wood post guardrail system was constructed with 7-inch (178 mm) diameter round wood posts substituted for the W6×9 (W150×14) steel posts. The 7-inch (178 mm) diameter round wood post was selected over a 6 inch × 8 inch (152 mm ×

203 mm) wood post because it has less flexural capacity and, thus, is more likely to fracture when confined within a mow strip.

The tests followed the impact conditions of *NCHRP Report 350* test 3-11, which involves a 4405-lb (2000 kg) pickup truck impacting the guardrail at a speed of 63 mph (100 km/h) and an angle of 25 degrees. In both tests, the vehicle was successfully contained and redirected in a stable manner. The grout material in the leave-out sections surrounding the posts failed as designed, permitting the posts in the impact region to rotate in the soil and help dissipate the lateral energy of the vehicle. A partial tear was observed in the W-beam rail after the steel post guardrail test, but the rail maintained its integrity and did not rupture. Two posts fractured during the wood post test, but the vehicle did not pocket into or rupture the rail. Although a couple of the posts contacted the back edge of the leave-out during testing, there was no damage to the concrete mow strip in either test. The repair would consist of removing the damaged guardrail components and grout, and resetting the system within the existing leave-outs. In summary, both guardrail systems met all the required evaluation criteria of *NCHRP Report 350* and demonstrated low maintenance/repair costs under design impact conditions.

CONCLUSIONS AND RECOMMENDATIONS

The performance of guardrails encased in pavement mow strip was researched using component tests, component simulations, predictive full-scale simulations, and full-scale crash testing. Nonlinear finite element analysis was an integral part of the design and evaluation process, and was used successfully in a predictive manner to select a mow strip design for both steel and wood post guardrail systems that achieved both the desired impact and maintenance performance. Two full-scale crash tests were successfully conducted in accordance with *NCHRP Report 350* to verify the impact performance of both steel post and wood post guardrail systems encased in a concrete mow strip with grout-filled leave-outs around the posts. Both guardrail systems met all the required evaluation criteria of *NCHRP Report 350* and demonstrated low maintenance/repair costs under design impact conditions.

The grout material in the leave-out sections surrounding the posts was a critical design element. Failure of the grout during impact permitted the posts in the impact region to rotate in the soil and help dissipate the lateral energy of the vehicle. Although a couple of the posts contacted the back edge of the leave-out during testing, there was no damage to the concrete mow strip in either test.

Any increase in post confinement beyond that provided by the grout backfill material used in the leave-out sections formed around the guardrail posts should be further evaluated. This applies to systems featuring guardrail posts directly encased in concrete or asphalt. In addition to providing greatly enhanced impact performance, it is believed that mow strip configurations featuring leave-outs are also more practical based on ease of repair after an impact.

CHAPTER 5. IMPLEMENTATION STATEMENT

In recent years, roadside safety research efforts have focused on the utilization of computer simulation technology to gain a better understanding of the behavior of roadside safety devices when subjected to vehicular impact. The main focus of this research is the application of finite element analysis (FEA) to the design and evaluation of improved roadside hardware. Three distinct roadside safety issues were investigated. This chapter presents implementation recommendations associated with each of these research areas.

T6 BRIDGE RAIL

The Texas T6 bridge rail is a breakaway bridge rail system that is designed for use on culvert headwalls and thin bridge decks. In full-scale crash testing, the Texas T6 bridge rail system did not satisfy *NCHRP Report 350* criteria for Test Level 3. Although the bridge rail contained and redirected the vehicle, the vehicle rolled onto its left side as it exited the installation.

A finite element model of the Texas T6 bridge rail system was developed to capture the performance trends of the existing T6 bridge rail system and evaluate potential design modifications. The goal is to achieve a system that will meet *NCHRP Report 350* criteria without significantly altering the basic design concept of the system (i.e., a relatively flexible, breakaway design capable of being installed on thin deck structures and culverts). Proposed modifications to the T6 system include revision of the breakaway post attachment detail and incorporation of a tubular thrie-beam rail element instead of the original tubular W-beam. During computer simulation of this alternative, the vehicle experienced significantly less roll angle and was inherently more stable than in the comparable simulation with the tubular W-beam rail element. The results suggest that the tubular thrie-beam system has a high probability of passing *NCHRP Report 350* Test Level 3 requirements.

The performance of the tubular thrie-beam system could be improved prior to testing by redesigning the post baseplate connection to increase its strength. The strength values should be chosen to reduce the number of posts broken to a total of six or seven posts. This would limit travel of the vehicle over the edge of the deck, which might further reduce the vehicle roll angle. Maintenance and repair costs would also be reduced.

GRID-SLOT PORTABLE CONCRETE BARRIER

The crash performance of the TxDOT Type 2 precast concrete traffic barrier (PCTB[1]-90) with joint type A was unproven with respect to the *NCHRP Report 350* guidelines. TTI researchers and TxDOT engineers worked together to evaluate the crash performance of this barrier system and determine if cost-effective modifications can be made to the barrier to meet *NCHRP Report 350* criteria and limit dynamic deflections to practical levels.

During the project, several retrofit connection designs were conceptualized for the objective of reducing dynamic barrier deflections. TxDOT engineers and TTI researchers developed these design modifications jointly. When developing these retrofit design options, factors such as impact performance, cost, ease of field installation, and aesthetics were considered. The research team performed computer simulations to help assess the ability of the selected retrofit connections to meet *NCHRP Report 350* impact performance criteria prior to conducting the full-scale crash testing. Limitations in the ability of existing material models to accurately capture concrete fracture and failure led to some simplifying assumptions regarding the model of the grid-slot connection. Nonetheless, the simulations assisted in the impact performance evaluation of the existing and modified designs.

Simulations and crash tests have indicated that the existing rebar grid connector is not capable of limiting the dynamic barrier deflections to reasonable levels under design impact conditions. A steel strap bolted to the toe of the barrier across the joint between adjacent barrier segments is considered to be the best retrofit alternative for limiting barrier deflections from among the three connections investigated. This connection limited the barrier deflection to only 4 ft (1.2 m) compared to the steel plate connector and U-bar connector, which had deflections of 9 ft (2.7 m) and 12.4 ft (3.8 m), respectively.

Subsequent to the crash test of this system, additional simulations were conducted to optimize the size of the steel strap. It was observed in the crash test of this connection detail that one of the steel straps failed in tension on the field side of the barrier. If the strength of the connection can be further increased to avoid failure of the strap without inducing failure of the anchor bolts, the barrier deflection can be further decreased. It was determined that if the size of the steel strap is increased to 6 inches (152 mm) wide × 1/4-inch (6 mm), tensile failure of the strap can be avoided and barrier deflections will be reduced to approximately 3.25 ft (1.0 m). Besides the change in plate dimensions, all other details of the connection, including anchor bolt size and location, remain the same as those used in the test installation. Since this reduction in deflection can be achieved with only a small increase in material cost, it is recommended that the 6-inch (152 mm) wide × 1/4-inch (6 mm) thick steel straps be implemented when site conditions cannot accommodate the larger deflections associated with the drop-in plate or grid connectors.

GUARD FENCE ENCASED IN MOW STRIP

The results of a full-scale simulation of a guard fence system encased in a solid concrete mow strip without leave-out sections around the posts indicated a low probability that such a system will meet *NCHRP Report 350* criteria. Researchers recommended that such practice be discontinued.

Additional simulations indicated that impact performance should be acceptable when an 18 inch × 18 inch (457 mm × 457 mm) leave-out section was provided around the posts and backfilled in the top 4 inches (102 mm) with a 2-sack grout mixture. The grout is effective in preventing vegetation growth, but crushes and permits rotation of a guardrail post during a guardrail impact. Predictive crash simulations of guard fence system models with this mow strip configuration indicated a high probability of meeting *NCHRP Report 350* guidelines. This was confirmed in subsequent full-scale crash tests conducted under Research Project 0-4162.

The successfully tested mow strip systems have been successfully implemented through preparation of a new standard detail sheet by TxDOT's Design Division. In addition to providing greatly enhanced impact performance, it is believed that mow strip configurations featuring leave-outs are also more practical based on ease of repair after an impact.

Any increase in post confinement beyond that provided by the grout backfill material used in the leave-out sections formed around the guardrail posts should be further evaluated. Additional guidance on acceptable mow strip variations is contained in Research Report 0-4162-2 *(10)*.

REFERENCES

1. Hallquist, J. O. *LS-DYNA3D Keyword User's Manual, Version 940*, Livermore Software Technology Corporation, Livermore, California, 1997.
2. Ross, H. E., D. Sickling, R. Zimmer, and J. Michie. *NCHRP Report 350: Recommended Procedures for the Safety Performance Evaluation of Highway Features*. TRB, National Research Council, Washington, D.C., 1993.
3. Hirsch, T. J., J. Panak, and C. Buth. *Tubular W-beam Bridge Rail*. Research Report 230-1. Texas Transportation Institute, Texas A&M University, College Station, Texas, October 1978.
4. Michie, J. D. *NCHRP Report 230: Recommended Procedures for the Safety Performance Evaluation of Highway Appurtenances*. TRB, National Research Council, Washington, D.C., March 1981.
5. Buth, C. E., R. Bligh, and W. Menges. *NCHRP Report 350 Test 3-11 of the Texas Type 6 Bridge Rail.* Report FHWA/TX-98/1804-4. Texas Transportation Institute, Texas A&M University, College Station, Texas, July 1998.
6. Reid, J. D. and D. L. Sicking. *Design of the SKT-350 Using LS-DYNA3D.* Transportation Research Board, 77th Annual Meeting, Washington, D.C., January 11-15, 1997.
7. Buth, C. E., W. F. Williams, R. Bligh, and W. Menges. *NCHRP Report 350 Test 3-11 of the Modified Texas Type 6 Bridge Rail on Bridge Deck.* Report FHWA/TX-00/1804-10. Texas Transportation Institute, Texas A&M University, College Station, Texas, February 2000.
8. "Public Finite Element Model Archive: Vehicle models," Federal Highway Administration/National Highway Transportation Safety Administration, National Crash Analysis Center, Washington, D.C., http://www.ncac.gwu.edu/archives/model/index.html, 2002.
9. Bligh, R. P., D. L. Bullard, Jr., W. L. Menges, and B. G. Butler. *Evaluation of Texas Grid-Slot Portable Concrete Barrier System.* Report FHWA/TX-02/4162-1. Texas Transportation Institute, Texas A&M University, College Station, Texas, April 2002.
10. Bligh, R. P., N. R. Seckinger, A. Y. Abu-Odeh, P. N. Roschke, W. L. Menges, and R. R. Haug, *Testing and Evaluation of TxDOT Mow Strips for Guardrails*, Report FHWA/TX-04/0-4162-2. Texas Transportation Institute, Texas A&M University, College Station, Texas, January 2004.
11. Eskandarian, A., D. Marzougui, and N. E. Bedewi (1997). "Finite Element Model and Validation of a Surrogate Crash Test Vehicle for Impacts with Roadside Objects," International Journal of Crashworthiness, 2(3), pp. 37-50.
12. Drucker, D. C., and W. Prager, "Soil mechanics and plastic analysis or limit design," *Quarterly of Applied Mathematics*, Vol. X, No. 2, 1952, pp. 157-165.
13. Hamilton, M. E., "Simulation of the T6 Bridge Rail Using LS-DYNA," MS thesis, Texas A&M University, College Station, Texas, 1999.